Biochemistry

© Copyright 2001 by the American Chemical Society Volume 40, Number 37 September 18, 2001

Articles

The *Tetrahymena* Ribozyme Cleaves a 5′-Methylene Phosphonate Monoester ~10^2-fold Faster Than a Normal Phosphate Diester: Implications for Enzyme Catalysis of Phosphoryl Transfer Reactions†

Xiangmin Liao,[‡,§] P. S. R. Anjaneyulu,[‡] Jessica F. Curley,[‡] Michael Hsu,[‡] Markus Boehringer,[⊥,||] Marvin H. Caruthers,[⊥] and Joseph A. Piccirilli*[,‡]

Howard Hughes Medical Institute, Departments of Biochemistry and Molecular Biology and of Chemistry, The University of Chicago, 5841 South Maryland Avenue, MC 1028, Chicago, Illinois 60637, and Departments of Chemistry and Biochemistry, University of Colorado at Boulder, Boulder, Colorado 80309

Received April 19, 2001; Revised Manuscript Received June 28, 2001

ABSTRACT: Single-atom substrate modifications have revealed an intricate network of transition state interactions in the *Tetrahymena* ribozyme reaction. So far, these studies have targeted virtually every oxygen atom near the reaction center, except one, the 5′-bridging oxygen atom of the scissile phosphate. To address whether interactions with this atom play any role in catalysis, we used a new type of DNA substrate in which the 5′-oxygen is replaced with a methylene (−CH_2−) unit. Under $(k_{cat}/K_m)^S$ conditions, the methylene phosphonate monoester substrate dCCCUCUT$_{mp}$TA_4 (where mp indicates the position of the phosphonate linkage) unexpectedly reacts ~10^3-fold faster than the analogous control substrates lacking the −CH_2− modification. Experiments with DNA−RNA chimeric substrates reveal that the −CH_2− modification enhances docking of the substrates into the catalytic core of the ribozyme by ~10-fold and stimulates the chemical cleavage by ~10^2-fold. The docking effect apparently arises from the ability of the −CH_2− unit to suppress inherently deleterious effects caused by the thymidine residue that immediately follows the cleavage site. To analyze the −O− to −CH_2− modification in the absence of this thymidine residue, we prepared oligonucleotide substrates containing methyl phosphate or ethyl phosphonate at the reaction center, thereby eliminating the 3′-terminal TA_4 nucleotidyl group. In this context, the −O− to −CH_2−modification has no effect on docking but retains the ~10^2-fold effect on the chemical step. To investigate further the stimulatory influence on the chemical step, we measured the "intrinsic" effect of the −O− to −CH_2− modification in nonenzymatic reactions with nucleophiles. We found that in solution, the −CH_2− modification stimulates chemical reactivity of the phosphorus center by <5-fold, substantially lower in magnitude than the stimulatory effect in the catalytic core of the ribozyme. The greater stimulatory effect of the −CH_2− modification in the active site compared to in solution may arise from fortuitous changes in molecular geometry that allow the ribozyme to accommodate the phosphonate transition state better than the natural phosphodiester transition state. As the −CH_2− unit lacks lone pair electrons, its effectiveness in the ribozyme reaction suggests that the 5′-oxygen of the scissile phosphate plays no role in catalysis via hydrogen bonding or metal ion coordination. Finally, we show by analysis of physical organic data that such interactions in general provide little catalytic advantage to RNA and protein phosphoryl transferases because the 5′-oxygen undergoes only a small buildup of negative charge during the reaction. In addition to its mechanistic significance for the *Tetrahymena* ribozyme reaction and phosphoryl transfer reactions in general, this work suggests that phosphonate monoesters may provide a novel molecular tool for determining whether the chemical step limits the rate of an enzymatic reaction. As methylene phosphonate monoesters react modestly faster than phosphate diesters in model reactions, a similarly modest stimulatory effect on an enzymatic reaction upon −CH_2− substitution would suggest rate-limiting chemistry.

One approach to understanding protein- and RNA-catalyzed phosphoryl transfer reactions has been to study the effects of substituting the oxygen atoms near the reaction center with other atoms or functional groups. In the case of

10.1021/bi010801u CCC: $20.00 © 2001 American Chemical Society
Published on Web 08/23/2001

the *Tetrahymena* ribozyme reaction, this approach has revealed an intricate network of transition state interactions (Figure 1) that enable the ribozyme to catalyze phosphoryl transfer with an $\sim 10^{11}$-fold rate acceleration (ref *6* and references therein). In this phosphoryl transfer reaction, nucleophilic attack by an exogenous guanosine (G) induces site specific cleavage of an oligonucleotide substrate (S).[1] The substrates, G and S, provide several ligands in the transition state for three active site metal ions (Figure 1) (*7*). M_A interacts with the 3′-oxygen leaving group of U^{-1} (*8*); M_B interacts with the 3′-oxygen nucleophile of G (*9*), and M_C interacts with the 2′-hydroxyl group of G (*7*, *10*). Additionally, M_A and M_C share a ligand in the transition state, the *pro-*S_p oxygen of the scissile phosphate (*6*, *11*). Together, these metal ions participate in catalysis to activate the nucleophile (M_B) and stabilize the negative charge that develops on the leaving group (M_A) and the phosphoryl group (M_A and M_C) in the transition state. The 2′-hydroxyl group of U^{-1} also plays an important role in catalysis but not as a ligand for a metal ion. As part of a hydrogen bond (H-bond) network with the 2′-hydroxyl group of A^{207} and the exocyclic amine of G^{22} (*12*), the 2′-hydroxyl group of U^{-1} donates an H-bond to the 3′-oxygen leaving group in the transition state, presumably acting in conjunction with M_A to stabilize the developing negative charge (Figure 1) (*13*, *14*).

So far, all of the outlined oxygen atoms in Figure 1 have been subjected to atomic mutagenesis except one, the bridging 5′-oxygen (O_{tg}; Figure 1) of the scissile phosphate, which is expected to occupy an equatorial position in the trigonal bipyramidal transition state. Could interactions with this atom play any role in the ribozyme-catalyzed reaction? To address this question and thus define further the interactions at the reaction center, we used a new type of ribozyme substrate containing a phosphonate monoester at the cleavage site, in which the 5′-bridging oxygen is replaced with a methylene ($-CH_2-$) group. As a $-CH_2-$ group can neither donate nor accept an H-bond or coordinate to a metal ion, a severely deleterious effect on the ribozyme reaction could implicate the 5′-oxygen in such a role. In contrast, the lack of a deleterious effect would provide evidence against H-bond interactions or metal ion coordination to the 5′-oxygen.

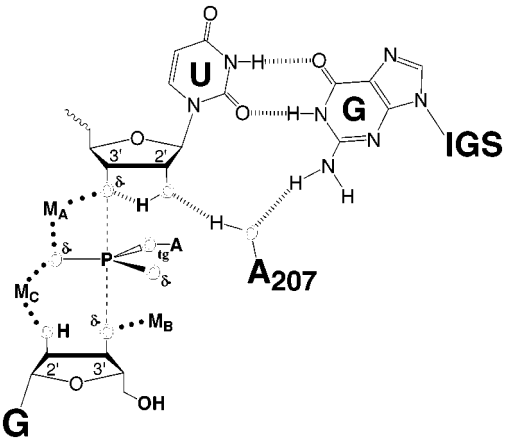

FIGURE 1: Model for the transition state interactions in the *Tetrahymena* ribozyme reaction. The dashed lines (- - -) depict the partial bonds between the reactive phosphorus, the leaving group and the incoming nucleophile, and $\delta-$ depicts the partial negative charges on the leaving group, the nucleophile, and the nonbridging phosphoryl oxygen atoms of the scissile phosphate. M_A is the metal ion coordinating the 3′-bridging oxygen of S (*8*). M_B is the metal ion coordinating the nucleophilic 3′-oxygen of G (*9*). M_C is the metal ion coordinating the 2′-hydroxyl of G (*7*, *10*). M_A and M_C both coordinate to the *pro-*S_p oxygen of the reactive phosphoryl group (*6*, *14*). Each of the outlined oxygen atoms has succumbed to atomic mutagenesis. This work addresses whether there are any transition state interactions with O_{tg}, the 5′-bridging oxygen atom of the transferred phosphoryl group.

Phosphonate esters are similar to phosphate esters except that one or more of the phosphorus−oxygen bonds is replaced with a phosphorus−carbon bond. An extensive body of literature describes the preparation and use of phosphonates as analogues of naturally occurring phosphates, including inorganic pyrophosphate, carbohydrate phosphates, nucleotides, and the phosphate products of glycolysis and phospholipid processing (*15*). With regard to nucleic acids, the phosphonates that mimic the phosphodiester backbone most closely fall into two categories: (1) methyl phosphonates, in which a methyl group replaces a nonbridging (nonesterified) oxygen atom, and (2) methylene phosphonates, in which a $-CH_2-$ group replaces a bridging (esterified) oxygen atom. The methyl phosphonate oligonucleotides have received the most attention because of their potential as antisense drugs and their ready synthetic accessibility via oligonucleotide synthesis. These oligonucleotide analogues retain the ability to form Watson−Crick duplexes (*16*), yet compared to natural nucleic acids, they resist digestion by nucleases and cross membranes more readily due to the neutral character of the phosphodiester backbone (*17*). The neutral character of the backbone also provides a useful tool

† J.F.C. was supported in part by the Molecular and Cellular Biology Training Grant (5T32GM07183) and the Medical Scientist Training Program (2T32GM07281). J.A.P. is an Associate Investigator of the Howard Hughes Medical Institute.

* To whom correspondence should be addressed. Phone: (773) 702-9312. Fax: (773) 702-0271. E-mail: jpicciri@midway.uchicago.edu.

‡ The University of Chicago.

§ Current address: Department of Medicinal Chemistry, SmithKline Beecham Pharmaceuticals, 709 Swedeland Rd., King of Prussia, PA 19406-0939.

‖ Current address: Pharma Research Basel Discovery Chemistry, F. Hoffman-LaRoche Ltd., PRBC-M Building 15/136, Basel CH4070, Switzerland.

⊥ University of Colorado at Boulder.

[1] Abbreviations: E, L-21 *Sca*I ribozyme; S, oligonucleotide substrate without specification of sequence; IGS, internal guide sequence at the 5′-end of the ribozyme (5′-GGAGGGA); G, guanosine; pG, guanosine 5′-monophosphate; E·S, bimolecular complex of ribozyme and substrate; E^G, bimolecular complex of ribozyme and guanosine; O_{tg}, 5′-bridging oxygen of the transferred phosphoryl group; Tris, tris(hydroxymethyl)aminomethane; MES, 2-(*N*-morpholino)ethanesulfonic acid; EDTA, ethylenedinitrilotetraacetic acid; MNP, triethylammonium 4-nitrophenyl methyl phosphate; ENP, triethylammonium 4-nitrophenyl ethyl phosphonate; PAGE, polyacrylamide gel electrophoresis; $t_{1/2}$, half-life. Substrates are named dS_{NN} or cS_{NN}, where d indicates all deoxyribose residues, c indicates a DNA−RNA chimeric oligonucleotide containing ribose residues at positions −2 and −3 and, if present, positions +2 to +5, NN indicates the identity of the residues or chemical entities flanking the reactive phosphoryl group, and mp represents a 5′-deoxy-5′-methylenephosphonate linkage. Thus, dCCCUC**UA**AAAA is represented as dS_{UA}, dCCCUC**TT**AAAA as dS_{TT}, dCCCUC$\mathbf{T_{mp}T}$AAAA as dS_{TmpT}, d(CCC)r(UC)d(**TT**)r(AAAA) as cS_{TT}, and d(CCC)r(UC)d($\mathbf{T_{mp}T}$)r(AAAA) as cS_{TmpT}. The chimeric substrate d(CCC)r(UC**U**)d**T**r(AAAA), which also contains a ribose residue at position −1, is represented as cS_{rUT}. Oligonucleotides dCCCUCT and d(CCC)r(UC)dT containing a 3′-terminal methyl phosphate are represented as dS_{TOCH_3} and cS_{TOCH_3}, respectively. Oligonucleotides dCCCUCT and d(CCC)r(UC)dT containing a 3′-terminal ethyl phosphonate are represented as $dS_{CH_2CH_3}$ and $cS_{CH_2CH_3}$, respectively.

Scheme 1: Strategy for the Synthesis of Oligonucleotides Containing a 3′-Terminal Methyl Phosphoryl or Ethyl Phosphonyl Group

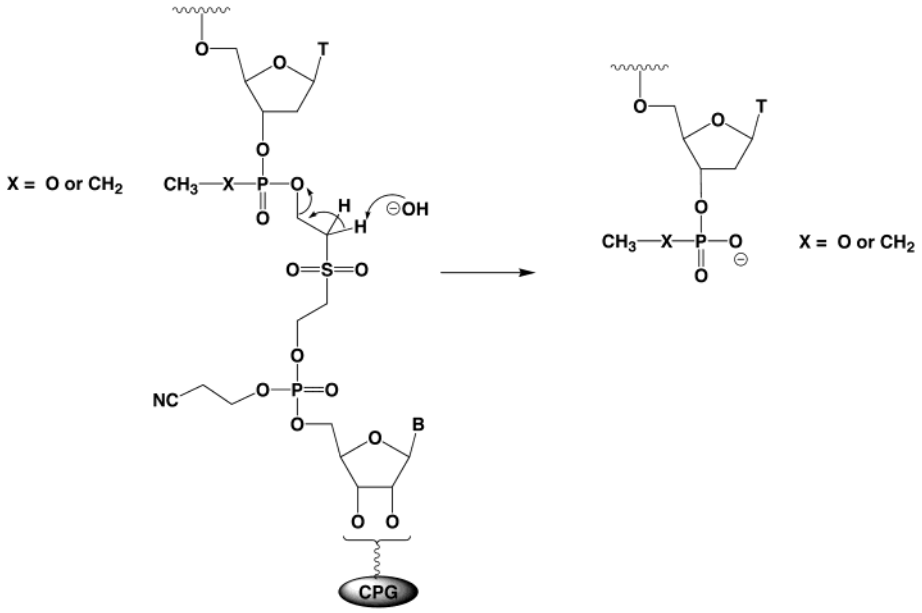

for exploring the importance of charge in the biological recognition of nucleic acids (*18*−*21*).

Less familiar and less accessible synthetically are oligonucleotides containing 3′- or 5′-methylene phosphonate monoester linkages, which, unlike the methyl phosphonates, are achiral and preserve the negative charge in the nucleic acid backbone (*22*, *23*). The limited data that are available suggest that oligonucleotides containing these linkages hybridize with stability similar to that of natural oligonucleotides and have little effect on helix conformation (*22*, *24*). Methylene phosphonate linkages resist cleavage by nucleases when the $-CH_2-$ unit replaces the oxygen leaving group in the reaction, providing useful inhibitors for structural studies of nuclease−substrate complexes (*25*). However, when the $-CH_2-$ substitution occurs at the other bridging oxygen, the phosphorus center may be susceptible to cleavage by enzymes. For example, Breaker et al. (*26*) obtained qualitative evidence that S1 nuclease and snake venom phosphodiesterase, enzymes that cleave the bond between the phosphorus and the 3′-oxygen, catalyze the hydrolysis of 5′-methylene phosphonate linkages in oligonucleotides.

In this work, we analyze quantitatively the reactivity of a ribozyme substrate containing a 5′-methylene phosphonate at the cleavage site and obtain for comparison the effect of the modification in nonenzymatic reactions. Our results show that the ribozyme cleaves the methylene phosphonate monoester substantially faster than the normal phosphate diester. This stimulatory effect of the $-CH_2-$ modification is greater than that which we observe in the nonenzymatic reactions, indicating that the ribozyme active site accommodates the phosphonate ester transition state more favorably than the normal phosphate diester transition state, possibly for geometric reasons. These results strongly suggest the absence of interactions between the ribozyme and the 5′-oxygen in the transition state. Estimates of the change in effective charge on the 5′-oxygen during the reaction imply that, in general, enzymes and ribozymes gain little catalytic advantage from H-bonding or metal ion coordination to the 5′-bridging oxygen during nucleotidyl transfer.

MATERIALS AND METHODS

Materials. Chemical reagents were purchased from Fisher Scientific or Aldrich Chemical Co. Nuclease S1 and T4 polynucleotide kinases were from U.S. Biochemicals. Guanosine (G) and guanosine 5′-monophosphate (pG) were from Sigma. [γ-^{32}P]ATP was from New England Nuclear, and phosphoramidites for solid-phase synthesis were from Glenn Research. The L-21 *Sca*I ribozyme was prepared by in vitro transcription using T7 RNA polymerase and purified as described previously (*27*); its concentration was determined by UV spectroscopy (*27*).

Oligonucleotide Synthesis, Purification, and Characterization. IGS′ oligonucleotide 5′-GGAGGG was a gift from D. Herschlag. Oligonucleotide substrates were synthesized according to standard procedures using β-cyanoethyl phosphoramidites. Oligonucleotides containing 5′-deoxy-5′-methylenephosphonate (mp)-linked thymidine ($dS_{T_{mp}T}$ and $cS_{T_{mp}T}$) were synthesized according to the method of Boehringer et al. (*22*) using the 3′-β-cyanoethyl phosphoramidite of a 5′-deoxy-5′-methylenephosphonate thymidine dimer ($T_{mp}T$). Solid-phase synthesis with this phosphoramidite dimer followed the same protocols as for the standard phosphoramidites except that the coupling time was 138 s. After solid-phase synthesis, the $T_{mp}T$ oligonucleotides and the corresponding control oligonucleotides (dS_{TT} and cS_{TT}) were treated with 0.5 M 2-nitrobenzaldoxime and tetramethylguanidine in a dioxane/H_2O mixture (3:1) to deprotect the phosphonate and cleave the oligonucleotide from the solid support (*22*). The mixtures were evaporated to dryness and treated with concentrated ammonium hydroxide to deprotect the heterocyclic bases. The all-phosphate-linked oligonucleotides deprotected in this way gave the same results as those deprotected by the standard ammonium hydroxide treatment.

Oligonucleotides containing a 3′-terminal methylphosphoryl group (dS_{TOCH_3} and cS_{TOCH_3}) or an ethylphosphonyl group ($dS_{TCH_2CH_3}$ and $cS_{TCH_2CH_3}$) were synthesized using the chemical phosphorylation reagent (Glenn Research) and thymidine

p-methoxyphosphoramidite (Chemgenes) or thymidine *p*-ethyl phosphoramidite (Chemgenes), respectively. The phosphorylating reagent was coupled to a synthesis column, followed by coupling of the appropriate thymidine phosphoramidite (Scheme 1). Subsequent synthetic and deprotection steps were carried out according to standard protocols.

The crude oligonucleotide samples were 5′-^{32}P-radiolabeled using [γ-^{32}P]ATP and T4 polynucleotide kinase. Denaturing PAGE followed by autoradiography showed that each sample contained several radiolabeled products. The correct oligonucleotide was tentatively identified by its migration relative to standards of known sequence. The appropriate band was excised from the gel, eluted into TE buffer [10 mM Tris and 1 mM EDTA (pH 7.5)], and butanol precipitated. The sample was dissolved in TE, desalted using a C-18 Sep-Pak cartridge, evaporated to dryness, and redissolved in TE. The concentrations of the 5′-^{32}P-labeled oligonucleotides were estimated by the specific radioactivity. The identity of each oligonucleotide was confirmed by digestion with S1 nuclease (Figures 3 and 4) and alkaline hydrolysis (for those containing ribonucleoside residues; Figure 4). HPLC purification of two oligonucleotides (cS_{TT} and $cS_{T_{mp}T}$) before 5′-radiolabeling did not change the kinetic results.

Kinetics of Ribozyme Reactions. Measurements were analogous to those described previously (*28*−*30*). All reactions were single-turnover with ribozyme in >10-fold excess of substrate and were carried out at 30 or 50 °C in a 10 μL volume containing ∼0.5 nM 5′-^{32}P-labeled substrate, 50 mM NaMES (pH 5.5 or 7.0), 10 mM $MgCl_2$, and G (or pG) (*28*). The same conditions were used for the site specific hydrolysis reaction, except that G (or pG) was omitted. Reaction conditions used to determine specific kinetic parameters are given in the footnotes of the tables. Reaction mixtures were preincubated without substrates at 50 °C for 30 min to renature the ribozyme. Substrate was incubated separately for 5 min at the temperature of the reaction. For reactions carried out at 30 °C, the preincubated ribozyme solution was transferred to a 30 °C water bath and incubated for 5 min before addition of substrate (*31*). Aliquots (1−2 μL) were withdrawn at specified times and the reactions quenched by dilution into 2 volumes of stop buffer (7.5 M urea, 20 mM EDTA, 0.1% xylene cyanol, and 0.1% bromophenol blue) followed by immediate cooling on dry ice. Substrates and products were separated by denaturing 20% PAGE. The fraction of substrate remaining at each time point [$S_t/(S_t + P_t)$, where S_t and P_t are the quantities of substrate and product, respectively, at a specific time t] was quantitated using a PhosphorImager (Molecular Dynamics). Plots of ln-[$S_t/(S_t + P_t)$] versus time were usually linear for approximately three half-lives and typically gave end points of ≥90%. Due to slow cleavage of dS_{TT} and dS_{UA}, rate constants for these reactions were measured from the initial rates.

Reactions of dS_{TT}, dS_{UA}, $dS_{T_{mp}T}$, dS_{TOCH_3}, and $dS_{TCH_2CH_3}$. Reactions were carried out at 30 °C, with ∼1 nM 5′-^{32}P-labeled substrates, 50 mM NaMES (pH 7.0), 10 mM $MgCl_2$, and 2 mM G using ribozyme concentrations of 10−1000 nM.

Reactions of DNA−RNA Chimeric Substrates cS_{TT}, $cS_{T_{mp}T}$, cS_{TOCH_3}, and $cS_{TCH_2CH_3}$. Reactions were carried out at 50 °C, with ∼1 nM 5′-^{32}P-labeled substrates, 50 mM NaMES (pH 7.0 or 5.5 as indicated), and 10 mM $MgCl_2$, with or without G (or pG) as indicated. At 50 °C and pH 7.0, the rates of cleavage of $cS_{T_{mp}T}$ at high ribozyme concentrations (≥100 nM) in the presence of saturating G (or pG) were too fast to measure accurately; thus, only the second-order rate constants $(k_{cat}/K_m)^S$ and $(k_{cat}/K_m)^G$ were measured under these conditions.

Scheme 2

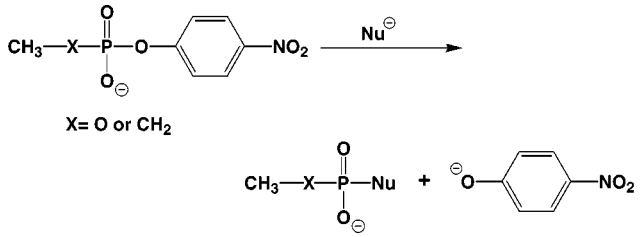

IGS′ Duplex Stability. To determine the affinity of binding of cS_{TT} and $cS_{T_{mp}T}$ to the IGS′ oligonucleotide (5′-GGAGGGA), we used the substrate inhibition assay described previously (*4*, *31*). Reactions were carried out at 50 °C, with ∼1 nM 5′-^{32}P-labeled substrates, 50 mM NaMES (pH 7.0), 10 mM $MgCl_2$, and 5 mM pG with 2 mM G using a ribozyme concentration of 100 (for cS_{TT}) or 0.5 nM (for $cS_{T_{mp}T}$). Concentrations of the ribozyme were chosen to ensure that reactions were under k_{cat}/K_m conditions. The concentration of IGS′ was varied from 0 to 100 μM.

Synthesis of Model Compounds. See the Supporting Information.

Kinetics of Reactions of MNP and ENP with Nucleophiles. Reactions of MNP and ENP at 25 °C were monitored spectrophotometrically (400 nm) by following the formation of 4-nitrophenoxide (Scheme 2). Reaction mixtures contained 0.1 mM substrate (triethylammonium salt of MNP or ENP) for reactions with hydroxide and ethanolamine, and 10 mM substrate for reactions with hydroxylamine. For hydroxylamine reactions, aliquots were removed at various times and diluted 10-fold with aqueous KOH before the absorbance at 400 nm was measured. For reactions with hydroxide, the ionic strength was maintained at 1.7 by addition of KCl, and the concentration of potassium hydroxide was varied from 0.3 to 1.7 M. Reactions with ethanolamine and hydroxylamine were carried out at pH 9.7 and 6.0, respectively, in the corresponding hydrochloride buffer (0.1−2 M); the ionic strength was maintained at 2.0 by addition of KCl. For each reaction, more than 10 time points were monitored. To determine end points, the reactions with 1.7 M hydroxide were monitored until the absorbance at 400 nm stopped increasing, ∼350 h for MNP and ∼180 h for ENP. The final absorbance (A_∞) for the reaction of each ester with hydroxide was used as the end point for all other reactions, including those in which ethanolamine or hydroxylamine was the nucleophile. Observed rate constants were determined from the slopes of plots of $\ln[(A_\infty - A_t)/A_\infty]$ versus time, where A_t is the absorbance at time t. Initial rates were used to determine the rate constants for the ethanolamine and hydroxylamine reactions. All reactions were first-order with time, and the second-order rate constants in Table 5 were obtained from plots of the observed rate constants versus nucleophile concentration. The second-order rate constant for the reaction of MNP with hydroxide (Table 5) is in good agreement with that reported by Rahil and Pratt [5.82×10^{-5} M^{-1} min^{-1} (*32*)].

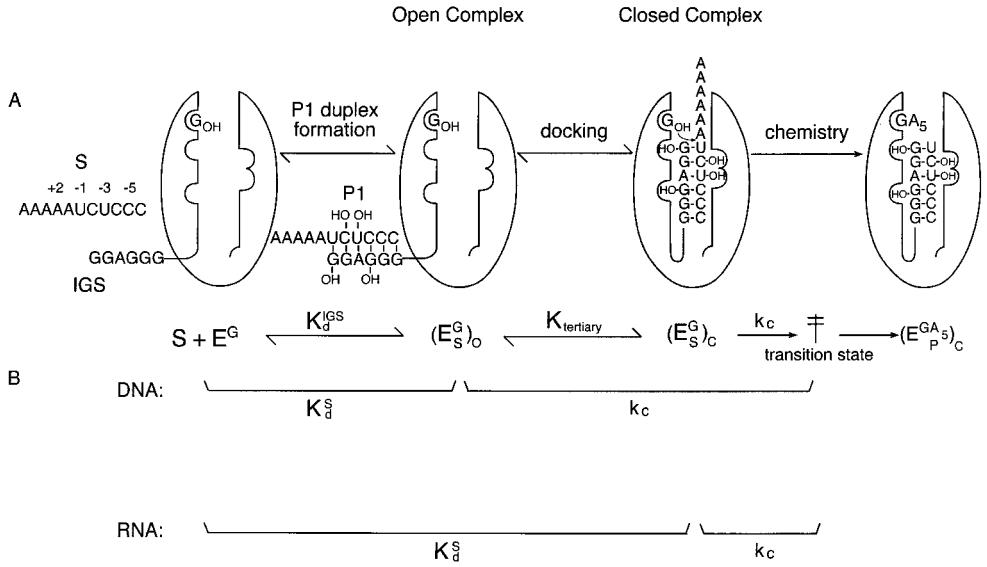

FIGURE 2: Endonuclease reaction catalyzed by the L-21 *Sca*I ribozyme (E). (A) The pathway for the reaction of the oligonucleotide substrate (CCCUCUAAAAA) with saturating guanosine (G) is shown. Binding of S is a two-step process (*36*−*38*). S first forms the open complex $(E^G{\cdot}S)_o$ by base pairing with the internal guide sequence (IGS, GGAGGG) of the ribozyme (E) to give the P1 duplex. The P1 duplex then docks into the catalytic core via tertiary interactions to form the closed complex $(E^G{\cdot}S)_c$ (*4*, *31*, *36*, *38*−*47*). Four of the 2′-OH groups involved in tertiary stabilization [located at G^{22} and G^{25} of the IGS (*43*) and at C^{-2} and U^{-3} of the substrate] are represented by −OH on the P1 duplex. The kinetic and thermodynamic parameters have been defined previously (*28*, *30*). K_d^{IGS} is the equilibrium constant for dissociation of S from $(E^G{\cdot}S)_o$. $K_{tertiary}$ is the equilibrium constant for docking into the tertiary interactions to form the closed complex. The chemical cleavage step (k_c) involves nucleophilic attack at the scissile phosphate diester by the 3′-hydroxyl group of a bound guanosine nucleoside (G). (B) The chemical step rate constant (k_c) and the equilibrium constant for dissociation of S from $E^G{\cdot}S$ (K_d^S) reflect different elementary steps for RNA and DNA substrates (*4*, *28*, *30*, *36*, *39*). For the DNA substrate, S binds in the open complex and, thus, $K_d^S = K_d^{IGS}$, while the rate constant k_c represents both the docking and chemical steps (*4*, *30*, *38*, *39*). For substrates containing 2′-OH groups at C^{-2} and U^{-3}, S binds in the closed complex and thus K_d^S represents both duplex-forming (K_d^{IGS}) and docking ($K_{tertiary}$) steps, while the rate constant k_c represents the chemical cleavage step (*4*, *36*, *38*, *39*, *51*).

Alkaline hydrolysis of MNP also was monitored by ^{1}H NMR (Brucker DMX 500 spectrometer, 500 MHz). Reaction conditions were the same as those used for UV measurements, except that the MNP concentration was 10 mM and the solvent was D_2O. Reactions were followed by integration of the *O*-methyl resonance of the starting diester (doublet at δ 3.73 relative to water) and that of the product monoester, methyl phosphate (doublet at δ 3.12). ^{1}H NMR showed that 4-nitrophenolate anion and methyl phosphate were the only products formed in the reaction. After alkaline hydrolysis was completed, ^{31}P NMR showed that the single ^{31}P resonance of the starting material (δ 3.18 relative to aqueous phosphoric acid) was completely converted to a single resonance (δ 5.66) of the methyl phosphate product. Plots of $\ln[S_t/(S_t + P_t)]$ versus time were linear for more than three half-lives. The second-order rate constant for the reaction of MNP with hydroxide obtained by NMR was in good agreement with that obtained by UV spectroscopy (Table 5).

Some nucleophiles, including hydroxide, react with phenyl phosphate esters or phenyl phosphonate esters via two pathways: (1) $S_N2(P)$ attack at phosphorus or (2) nucleophilic aromatic substitution at C1 of the phenyl ring (*2*, *33*). The observed rates of the reaction of MNP and ENP with nucleophiles could therefore represent the sum of the rates for both pathways. Because the rate for attack of nucleophiles at phosphorus is of interest for this work, it is necessary to determine the contribution of each pathway to the overall rate of reaction. ^{31}P NMR product analysis (*33*) of reactions with [^{18}O]hydroxide ion shows that the ratio of [^{16}O]methyl phosphate to [^{18}O]methyl phosphate or [^{16}O]ethyl phosphonate to [^{18}O]ethyl phosphonate is not detectably different from the ratio of ^{16}O to ^{18}O in the solvent. These results indicate that reactions of both MNP and ENP with hydroxide occur predominantly through attack at phosphorus. To address the contribution by the amine nucleophiles to each pathway, we monitored the reactions of 2 M ethanolamine (pH 9.7) or hydroxylamine (pH 6.0) with 10 mM MNP by ^{1}H NMR over a period of 167 days. During this period of time, >60% of the MNP reacts with ethanolamine, and >90% with hydroxylamine. ^{1}H NMR showed only the formation of *p*-nitrophenol; we could detect no *p*-nitrophenylamines, which would result from attack at carbon. Thus, the second-order rate constants for the reactions of the amine nucleophiles represent attack at phosphorus. This is consistent with the observation that a variety of amine nucleophiles show little or no tendency to react at the aromatic carbon of *p*-nitrophenyl methyl phosphonate (*1*).

RESULTS

The L-21 *Sca*I ribozyme, derived from the *Tetrahymena thermophila* self-splicing group I intron, catalyzes phosphoryl transfer between RNA or DNA substrates and guanosine (or one of its 5′-phosphorylated forms) in a reaction analogous to the first step of self-splicing (*28*, *30*, *34*, *35*).

$$\overset{-5}{C}\overset{-3}{C}\overset{-1}{C}\overset{+2}{U}CUAAAAA + G \xrightarrow{E} CCCUCU + GAAAAA \quad (1)$$

Water or hydroxide can replace G as the nucleophile in an

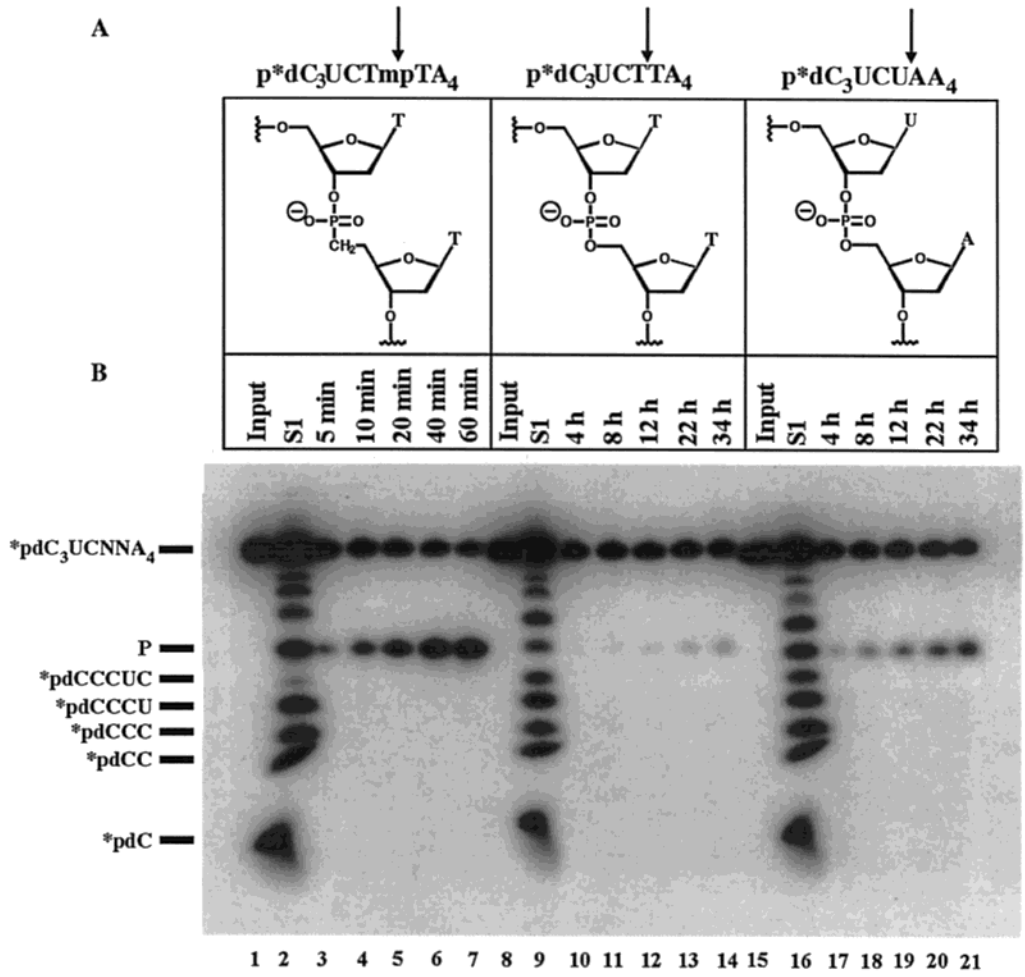

FIGURE 3: *Tetrahymena* ribozyme cleaves a DNA substrate containing a methylene phosphonate linkage at the scissile phosphorus center much faster than the natural phosphate diester linkage. (A) Structures of the DNA substrates used in this work (left, $dS_{T_{mp}T}$; center, dS_{TT}; right, dS_{UA}). The deoxyribose phosphate backbone at the cleavage site is shown to illustrate the chemical nature of the single-atom change. The "normal" substrates have phosphate diester linkages at all backbone positions, and the "mp" substrate has the 5′-methylene phosphonate monoester linkage at the cleavage site and phosphate diester linkages at all other sites. (B) Time course and product characterization for ribozyme reactions of the substrates shown in panel A. Reactions were carried out at 30 °C with 1000 nM E, 2 mM G, ~1 nM 5′-^{32}P-labeled DNA substrate as indicated, 50 mM NaMES (pH 7.0), and 10 mM $MgCl_2$. The products were identified as P (dCCCUCT for ribozyme cleavage of dCCCUCTmpTAAAA and dCCCUCTTAAAA and dCCCUCU for ribozyme cleavage of dCCCUCUAAAAA) by comparison with the ladders generated by partial digestion with S1 nuclease (lanes denoted by S1).

analogous sequence specific hydrolysis reaction (*28*). The binding of oligonucleotide substrate (S) to the ribozyme (E) involves two steps (Figure 2) (*36*−*38*). First, S interacts with E by complementary Watson−Crick base pairing with the internal guide sequence (IGS) to form an open E·S complex $(E{\cdot}S)_o$; then, the resulting P1 duplex docks into the ribozyme active core via tertiary interactions to form the closed complex $(E{\cdot}S)_c$ (*4*, *31*, *36*, *38*−*47*). Quantitative analysis of the reaction rate and equilibrium constants involved in this endonuclease reaction pathway has provided a kinetic and thermodynamic framework for understanding the energetics of catalysis and for interpreting the results of mutagenesis experiments (*28*−*30*, *48*−*51*).

The Ribozyme Cleaves a Phosphonate Monoester ~10^3-Fold Faster Than a Phosphate Diester. We synthesized an all-DNA substrate $dCCCUCT_{mp}TA_4$ ($dS_{T_{mp}T}$, Figure 3A) containing at the cleavage site two thymidine residues linked by a methylene phosphonate monoester. We used thymidine residues in place of the natural UA residues because of the availability of the 3′-phosphoramidite of the 5′-deoxy-5′-methylenephosphonate-linked thymidine dimer (*22*). Substitution of dT for dU at the cleavage site previously was shown to have little effect on the cleavage rate of normal DNA substrates (*28*, *44*). We also synthesized two control substrates: dS_{TT}, containing two thymidine residues linked by a normal phosphate diester, and dS_{UA}, the standard DNA substrate (Figure 3A). When the 5′-^{32}P-end-labeled substrates were incubated at 30 °C (pH 7.0) in the presence of 2 mM G and 1 μM L-21 *Sca*I ribozyme, the modified substrate $dS_{T_{mp}T}$ reacted almost completely within 1 h ($t_{1/2}$ ~ 0.5 h; Figure 3B, lanes 3−7), whereas the substrates containing the normal phosphate linkage, dS_{TT} and dS_{UA}, reacted much more slowly ($t_{1/2}$ ~ 640 h, lanes 10−14; and $t_{1/2}$ ~ 83 h, lanes 17−21). The product of ribozyme cleavage of $dS_{T_{mp}T}$ comigrated with that from dS_{TT} and with the appropriate product (*pdCCCUCT) from S1 nuclease digestion of $dS_{T_{mp}T}$ (lane 2) and dS_{TT} (lane 9), confirming that the ribozyme cleaves the substrate at the methylene phosphonate linkage.

We measured the dependence of k_{obsd} on the concentration of E for $dS_{T_{mp}T}$, dS_{TT}, and dS_{UA} and fit the data by nonlinear least-squares analysis to determine the kinetic parameters k_c and K_m (Table 1). For the standard DNA substrate, dS_{UA},

Table 1: Comparison of DNA Substrates Containing a Normal Phosphate Linkage or a 5′-Deoxy-5′-methylene Phosphonate Linkage at the Cleavage Site[a,b]

	substrate	k_{cat}/K_m[c] (M^{-1} min^{-1})	k_c ($\times 10^5$ [d] min^{-1})	k_c^{rel} [e]	K_d [f] (nM)	K_d^{rel} [g]
dS_{UA}	dC_3UCUA_5	1543	14	8	68	1.6
dS_{TT}	dC_3UCTTA_4	223	1.8	(1)	43	(1)
$dS_{T_{mp}T}$	$dC_3UCT_{mp}TA_4$	280000	2600	1400	61	1.4

[a] Reactions with 0−2000 nM ribozyme, 2 mM G, and ∼1 nM 5′-end-labeled substrate in 50 mM NaMES (pH 7.0 and 25 °C) and 10 mM $MgCl_2$ at 30 °C. G was shown to be near saturating for dS with a K_m(G) of ∼1 mM (*49*), and no correction for saturation was made. [b] The given values represent nonlinear least-squares fits to the data. [c] The second-order rate constant for the reaction of E^G and substrate (*30*). [d] The rate constant k_c is that for the chemical conversion of the $(E^G{\cdot}S)_o$ ternary complex (*39*). [e] $k_c^{rel} = k_c^{dS}/k_c^{dS_{TT}}$, representing the rate constant for cleavage of dS relative to that of dC_3UCTTA_4. [f] The equilibrium constant K_d for dissociation of S from the $E^G{\cdot}S$ complex. The values were obtained from nonlinear least-squares fits to plots of k_{obsd} vs E^G, assuming $K_m = K_d$. [g] $K_d^{rel} = K_d^{dS}/K_d^{dS_{TT}}$, representing the dissociation constant for dS relative to that of dC_3UCTTA_4.

K_m equals K_d, the equilibrium constant for dissociation of S from the open complex, $(E^G{\cdot}S)_o \leftrightarrows E^G + S$ (Figure 2B), and should therefore reflect the stability of the P1 duplex under the reaction conditions (*4*, *30*, *38*, *52*−*54*). The rate constant k_c represents both the docking and chemical steps. The values of K_d and k_c for $dS_{T_{mp}T}$, dS_{TT}, and dS_{UA} show that the unexpectedly fast cleavage rate of the methylene phosphonate linkage manifests itself only in k_c and not in K_d. The similar K_d values for the three substrates (within error) indicate that the substrates bind in the open complex with equal affinity (Table 1). Thus, the 5′-O to 5′-CH_2 substitution has little effect on the stability of the P1 duplex, consistent with the previous observation that a 5′-CH_2 modification does not affect oligonucleotide duplex stability (*26*). In contrast, the 5′-CH_2 modification in $dS_{T_{mp}T}$ increased k_c by (1.4×10^3)-fold relative to that of the control substrate dS_{TT} (Table 1), indicating 4.4 kcal mol^{-1} of transition state stabilization from the 5′-CH_2 substitution. Because k_c for DNA substrates reflects both the docking and chemical steps, the larger k_c value may arise from more favorable docking of the substrate into the closed complex and/or from faster chemistry.

The 8-fold smaller value of k_c for dS_{TT} compared to that for dS_{UA} (Table 1) was unexpected because previous work had shown that substitution of the deoxyuridine immediately preceding the cleavage site with thymidine (dS_{TA}) has no effect on activity (*30*) and because the adenine base of the residue immediately following the cleavage site (+1) putatively makes no tertiary interactions (*39*, *52*). We confirmed that dS_{TA} reacts as efficiently (within 40%) as dS_{UA} but found that dS_{UT}, in which the adenosine immediately following the cleavage site was substituted with thymidine, reacts ∼2.5-fold slower than dS_{UA}. Thus, the 8-fold lower reactivity of dS_{TT} compared to dS_{UA} appears to arise from the combination of T's, but we do not know the reason for this effect (see below). The modified postsynthetic workup involving treatment with 2-nitrobenzaldoxime and tetramethylguanidine (see Materials and Methods) does not cause the lower reactivity of dS_{TT}, as dS_{TT} prepared without this modified workup still reacts 8-fold slower than dS_{UA}.

To account for the strikingly favorable effect of the 5′-O to 5′-CH_2 substitution, we analyzed further the effect of this atomic perturbation in three ways. (1) We incorporated 2′-hydroxyl groups into the substrates so that we could observe differences in docking. (2) We studied the effect of the 5′-O to 5′-CH_2 substitution in the context of substrates in which the 3′-terminal residues (+1 to +5) were replaced with a methoxy ($-OCH_3$) and an ethyl group ($-CH_2CH_3$), respectively (Scheme 1). (3) We measured the intrinsic differences in the reactivity of a model phosphonate monoester and a phosphate diester toward nucleophiles.

Reactions with Chimeric DNA−*RNA Substrates*. The 2′-hydroxyl groups at positions U^{-3} and C^{-2} stabilize docking of the P1 duplex into the closed complex by factors of 65 and 18, respectively, and maintain this stabilization in the transition state for the chemical step (*4*, *39*, *40*). To determine whether these 2′-hydroxyl groups have a similar stabilizing effect on the cleavage reaction of the methylene phosphonate substrate and to attribute the faster cleavage rate of the methylene phosphonate substrate to effects on the docking versus the chemical step, we synthesized substrates containing 2′-hydroxyl groups at U^{-3} and C^{-2} (cS_{rUT}, cS_{TT}, and $cS_{T_{mp}T}$). Because the methylene phosphonate linkage had not been incorporated previously into an oligonucleotide containing ribose residues, we analyzed $cS_{T_{mp}T}$ by partial alkaline cleavage and S1 nuclease digestion (Figure 4). The ladders generated for $cS_{T_{mp}T}$ (lane 7) were similar to those for cS_{TT} (lane 11) and cS_{rUT} (lane 3). Additionally, the product that resulted from cleavage by the L-21 *Sca*I ribozyme (lane 8), presumably *pd(CCC)r(UC)dT, comigrated with the product from the cleavage of cS_{TT} (lane 12).

Ribozyme reactions were carried out at 50 °C so that we could determine P1 duplex stability under the same conditions using the method of substrate inhibition (*4*, *31*). As expected, the second-order rate constants for reactions at 50 °C and pH 7.0 of cS_{TT} and $cS_{T_{mp}T}$ with E^G (Table 2) increased by ∼2 orders of magnitude compared to those for their all-deoxy counterparts (dS_{TT} and $dS_{T_{mp}T}$, respectively), indicating that the 2′-hydroxyl groups at U^{-3} and C^{-2} contribute energetic stabilization in the transition state. For substrates lacking the 2′-hydroxyl at position −1, such as cS_{TT}, the rate-limiting step for $(k_{cat}/K_m)^S$ is chemical cleavage (*55*) so that $(k_{cat}/K_m)^S$ reflects the overall free energy difference for the reaction $E^G + S \rightarrow$ products. Under these conditions, $cS_{T_{mp}T}$ reacts ∼400-fold faster than cS_{TT} (data not shown). However, this comparison of $(k_{cat}/K_m)^S$ values for cS_{TT} and $cS_{T_{mp}T}$ could be misleading because different steps could be rate-limiting for each substrate (see below).

Determining the Effect of the 5′-O to 5′-CH_2 Substitution on the Energetics of Binding. The equilibrium dissociation constant for binding of S to E^G (K_d^S) equals K_m for S in the reaction with the E^G complex if S dissociates from the $E^G{\cdot}S$ complex much faster than the ternary complex ($E^G{\cdot}S$) reacts to give products, i.e., $k_{off} \gg k_c$. The reaction of cS_{TT} likely satisfies this condition because this substrate reacts very slowly (Table 2). However, $cS_{T_{mp}T}$ reacts with a $(k_{cat}/K_m)^S$ value (6.2×10^7 M^{-1} min^{-1}; Table 2) strikingly similar to the value of 10^8 M^{-1} min^{-1} for duplex formation (*28*, *36*, *51*), indicating that the 5′-CH_2 substitution might have accelerated the chemical step to the extent that binding of the oligonucleotide substrate to the IGS becomes rate-limiting. Therefore, K_m for $cS_{T_{mp}T}$ may not equal K_d, and the kinetic parameters for $cS_{T_{mp}T}$ and cS_{TT} should not be

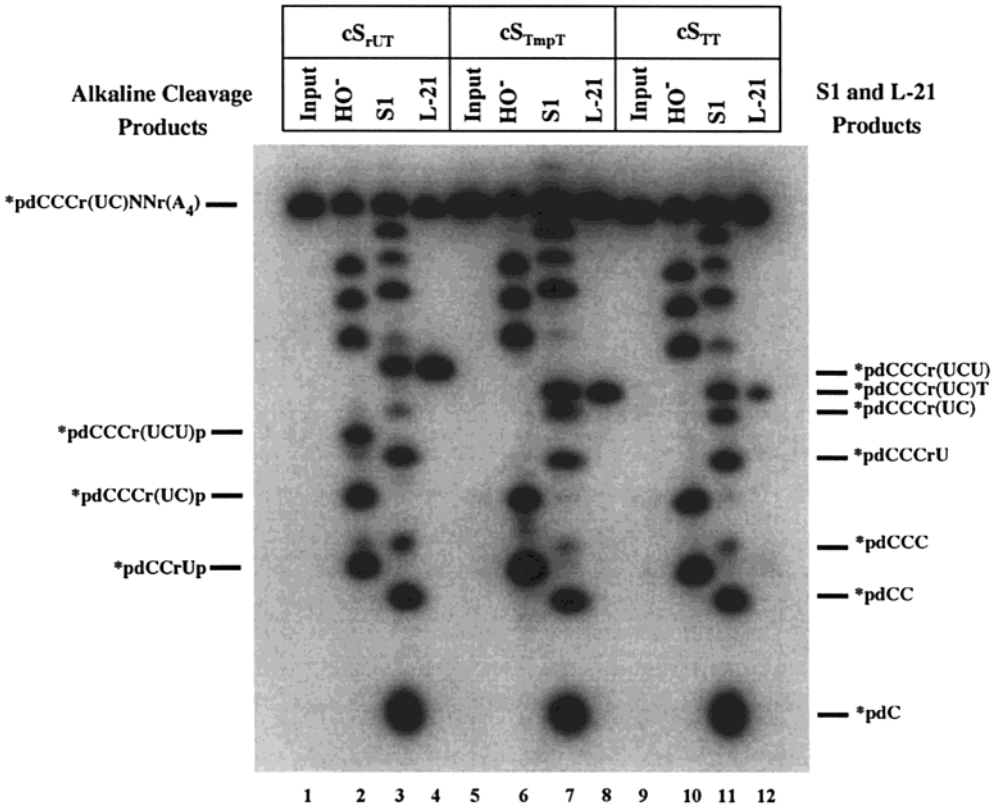

FIGURE 4: Ribozyme cleavage and characterization of chimeric DNA−RNA substrates d(CCC)r(UCU)Tr(AAAA) (cS$_{rUT}$), d(CCC)r(UC)-TmpTr(AAAA) (cS$_{T_{mp}T}$), and d(CCC)r(UC)TTr(AAAA) (cS$_{TT}$). Lanes are as follows: input, untreated 5′-^{32}P-labeled chimeric substrate; HO$^-$, partial alkaline hydrolysis of S obtained by treatment with 0.1 M $NaHCO_3$ (95 °C for 40 min); S1, partial digestion by S1 nuclease; L-21, ribozyme cleavage reaction after 1 min (cS$_{rUT}$ and cS$_{T_{mp}T}$) or 4 h (cS$_{TT}$). Ribozyme reactions were single-turnover reactions whose mixtures contained <1 nM radiolabeled substrate, 200 nM ribozyme, 50 mM NaMES, 5 mM pG, and 10 mM $MgCl_2$ at 50 °C and pH 5.5.

Table 2: Comparison of the Guanosine-Dependent Endonuclease Reactions of the Substrates in the Chimeric DNA−RNA Background[a]

	substrate	$(k_{cat}/K_m)^{S}$ [b] ($\times 10^7$ M^{-1} min^{-1})	$(k_{cat}/K_m)^{pG}$ [c] ($\times 10^4$ M^{-1} min^{-1})	K_d^{pG} [d] (μM)	k_c [e] (min^{-1})	k_c^{rel} [f]	K_d^{S} [g] (nM)	$K^{IGS'}$ [h] (nM)	$K_{tertiary}$ [i]	$K_{tertiary}^{rel}$ [f]
cS$_{TT}$	d(CCC)r(UC)d(TT)rA$_4$	0.015	0.0059	730	0.043	(1)	990	15100	15	(1)
cS$_{T_{mp}T}$	d(CCC)r(UC)dT$_{mp}$TrA$_4$	6.2	1.8	160	2.9	67	110	19900	190	12
cS$_{rUT}$	d(CCC)r(UCU)dTrA$_4$	7.8	1.4	4500	63	1465	160	37000	240	16

[a] Reactions were carried out with ~1 nM 5′-end-labeled substrate, 50 mM NaMES (pH 7.0 or 5.5 as indicated), and 10 mM $MgCl_2$ at 50 °C. [b] $(k_{cat}/K_m)^S$ is the second-order rate constant for the reaction of E^G and cS at pH 7.0 (*28*). The values were determined from nonlinear least-squares fits to plots of k_{obsd} vs [E]. Reactions were carried out with 5 mM pG and ribozyme (0−10 nM for cS$_{T_{mp}T}$ and cS$_{rUT}$ and 0−100 nM for cS$_{TT}$). [c] $(k_{cat}/K_m)^{pG}$ is the second-order rate constant for the reaction of the E·S complex and pG (*28*, *49*). The values were determined from nonlinear least-squares fits to plots of k_{obsd} vs [pG]. Reactions were carried out at pH 5.5 with 5 μM (for cS$_{TT}$) or 2 μM E (for cS$_{T_{mp}T}$ and cS$_{rUT}$) and 0−100 μM (for cS$_{TT}$) or 0−20 μM pG (for cS$_{T_{mp}T}$ and cS$_{rUT}$). [d] K_d^{pG} was obtained from nonlinear least-squares fits to plots of k_{obsd} vs [pG]. Reactions were carried out at pH 5.5 and 5 μM (for cS$_{TT}$) or 2 μM ribozyme (for cS$_{T_{mp}T}$ and cS$_{UT}$). [e] k_c, the rate constant for the chemical step, is determined from the second-order rate constant for the reaction of the E·S complex with pG and the dissociation constant for E·S and pG by the relationship $k_c = (k_c/K_m)^{pG} \times K_d^{pG}$ as previously described (*28*). It is assumed that the chemical cleavage step is rate-limiting for $(k_c/K_m)^{pG}$ and K_m^{pG} (pH 5.5) = K_d^{pG} (pH 7.0) (*4*, *49*). [f] k_c^{rel} and $K_{tertiary}^{rel}$ are values relative to those for cS$_{TT}$. [g] Reactions were carried out at pH 5.5 in the presence of 5 mM pG with 0−5 μM (for cS$_{TT}$) or 0−2 μM ribozyme (for cS$_{T_{mp}T}$ and cS$_{rUT}$). Values are nonlinear least-squares fits to plots of k_{obsd} vs [ribozyme]. K_m^S is the Michaelis constant for reactions of S with the E·G complex. It is assumed that at pH 5.5 $K_m^S = K_d^S$ and that K_d^S is the same at pH 5.5 and 7.0 (*4*, *51*). [h] $K^{IGS'}$ is the affinity of binding of the substrate to the IGS′ oligonucleotide (5′-GGAGGGA-3′) (*4*); reactions were carried out at 50 °C and pH 7.0 with 5 mM pG and 100 nM (for cS$_{TT}$) or 0.5 nM ribozyme (for cS$_{T_{mp}T}$ and cS$_{rUT}$). Concentrations of ribozyme were chosen to ensure that reactions were carried out under k_{cat}/K_m conditions. The concentration of IGS′ was varied from 0 to 100 μM. [i] $K_{tertiary}$ is the equilibrium constant for docking of the P1 duplex into the tertiary interactions with the core of the ribozyme in the presence of saturating pG and is calculated from the equation $K_d^S = K^{IGS'}/(1 + K_{tertiary})$ (*4*). It is assumed that K_d^S is the same at pH 5.5 and 7.0 (*4*, *49*, *51*).

compared directly. To circumvent this potential complication and to allow direct comparison of kinetic parameters, we carried out the reactions at pH 5.5. Herschlag and co-workers have shown that the chemical cleavage step increases with pH in a log-linear fashion (pH <7) (*13*, *56*) and that binding of both S and G is independent of pH (*49*, *51*, *53*). Thus, for RNA substrates, decreasing the pH to 5.5 renders the chemical step rate-limiting such that $K_m^S = K_d^S$ and $K_m^G = K_d^G$ (*13*, *28*, *49*, *55*, *56*). The K_m value measured at pH 5.5 therefore can be taken as the binding affinity at pH 7.0. We carried out reactions of cS$_{TT}$, cS$_{T_{mp}T}$, and cS$_{rUT}$ at pH 5.5 to determine affinities for binding of G to the E·S complex and of S to the E^G complex (Table 2). As expected, cS$_{TT}$ and cS$_{T_{mp}T}$ reacted at pH 5.5 more than 1 order of magnitude

slower than at pH 7.0. Plots of k_{obsd} versus E^G concentration were fit via nonlinear least-squares analysis and showed that $cS_{T_{mp}T}$ binds ~9-fold more strongly to E^G than does cS_{TT} (K_d^S = 110 vs 990 nM, respectively; Table 2).

To determine whether the greater binding affinity of $cS_{T_{mp}T}$ arises from the greater stability of the P1 duplex or to more favorable docking into the catalytic core of E^G, we assessed the binding of cS_{TT} and $cS_{T_{mp}T}$ to an IGS analogue using the method of substrate inhibition (*4*, *31*). The IGS analogue (GGAGGG, IGS′) binds to free S to form a P1 duplex analogue, preventing S from binding to E^G and undergoing reaction. The ability of IGS′ to inhibit the reaction of S and E^G under $(k_{cat}/K_m)^S$ conditions depends directly on the stability of the analogue P1 duplex and reflects the energetics of S binding to E^G in the open complex ($K^{IGS'}$). The similar $K^{IGS'}$ values of 15 and 20 μM for cS_{TT} and $cS_{T_{mp}T}$, respectively (Table 2), show that the methylene phosphonate linkage has no effect on P1 duplex stability, consistent with the results obtained in the DNA background (see above).

The energetics of docking of the P1 duplex into the catalytic core of E^G are given by $K_{tertiary}$ according to eq 2:

$$K_d^S = K^{IGS'}/(1 + K_{tertiary}) \quad (2)$$

where K_d^S is the dissociation constant for the overall equilibrium $E^G{\cdot}S \leftrightarrows E^G + S$ and $K^{IGS'}$ is as described above (*4*). Using eq 2 and the values of K_d^S and $K^{IGS'}$, we calculated $K_{tertiary}$ for cS_{TT} and $cS_{T_{mp}T}$ as 15 and 190, respectively (Table 2), indicating that the docking of $cS_{T_{mp}T}$ into the catalytic core is 12-fold more favorable than the docking of cS_{TT}.

Effect of the 5′-O to 5′-CH_2 Substitution on the Chemical Step. For substrates that bind to the ribozyme in the closed complex, the rate constant k_c describes the rate of chemical conversion of the $E^G{\cdot}S$ ternary complex to products (*28*, *30*, *55*). Because cS_{TT} reacts slowly, measuring the cleavage rate in the presence of saturating E and G gives k_c directly. In contrast, at pH 7 in the presence of saturating ribozyme and G, $cS_{T_{mp}T}$ reacts too fast to measure accurately. At low G concentrations, however, a step involving G, presumably the chemical step, becomes rate-limiting (*28*). Thus, for fast-reacting substrates such as the RNA substrate CCCUCUAAAAA, k_c can be calculated using the relationship

$$k_c = (k_{cat}/K_m)^{pG} K_d^{pG} \quad (3)$$

where $(k_{cat}/K_m)^{pG}$ is the second-order rate constant for the reaction of the E·S complex and pG and K_d^{pG} is the equilibrium constant for dissociation of pG from the $E^{pG}{\cdot}S$ ternary complex (*28*, *30*). We used this approach to obtain the k_c value for $cS_{T_{mp}T}$.

Reactions were carried out with saturating ribozyme and several different concentrations of pG. At low concentrations of pG, plots of k_{obsd} versus pG concentration gave good straight lines for each substrate, and the slopes of these lines are listed as $(k_{cat}/K_m)^{pG}$ values in Table 2. We determined K_d^{pG} (Table 2) by measuring the K_m for pG in the reaction of pG with the E·S complex at pH 5.5 and by assuming that $K_d^{pG} = K_m^{pG}$ (*49*). As indicated above, decreasing the pH slows the rate of chemistry (*13*, *31*, *39*) but has no effect on pG binding (*49*). Consistent with this observation, pG and the $E{\cdot}cS_{TT}$ complex react at pH 7 with the same K_m^{pG} value as at pH 5.5. Binding of G or pG to the ribozyme strengthens in the presence of substrates that favor the closed complex; i.e., G and pG bind to the $(E{\cdot}S)_c$ complex ~5-fold more strongly than to free E or the $(E{\cdot}S)_o$ complex (*49*). The literature values of K_d^{pG} for binding of pG to free E or the $(E{\cdot}S)_c$ complex [where S is CCCUC(dU)A; 30 °C and pH 5.5] are 320 and 90 μM, respectively (*49*). We obtained a K_d^{pG} value of 100 μM (pH 5.5) using the all-RNA substrate, CCCUCUAAAAA, which binds in the closed complex (*4*, *38*, *52*−*54*). A similar value of 160 μM (pH 5.5) was obtained using $cS_{T_{mp}T}$ as the substrate (Table 2), suggesting that $cS_{T_{mp}T}$ binds in the closed complex. With cS_{TT} as the substrate, however, binding of pG to the E·S complex was ~5-fold weaker [K_d^{pG} = 730 μM (pH 5.5); Table 2]. This observation together with the weaker binding of cS_{TT} than $cS_{T_{mp}\mathbf{T}}$ suggests that cS_{TT} may dock into the catalytic core only partially. Using eq 3 and values of $(k_{cat}/K_m)^{pG}$ and K_d^{pG}, the k_c values for cS_{TT} and $cS_{T_{mp}T}$ were calculated to be 0.043 and 2.9 min^{-1}, respectively (Table 2). The k_c value for cS_{TT} is the same within error as the value of 0.062 min^{-1} measured directly at pH 7.0 with saturating ribozyme and pG. The ratio of k_c values for cS_{TmpT} and cS_{TT} (2.9/.047 = 67) indicate that ~10^2-fold of the overall 10^3-fold effect arising from the $-CH_2-$ modification occurs during the chemical step.

For comparison, we determined the corresponding kinetic parameters for the DNA−RNA chimeric substrate containing a ribonucleoside at the cleavage site [cS_{rUT}; d(CCC)r(UCU)-dTr(AAAA); ribothymidine was not available]. As expected, this substrate reacts with k_c more than 10^3-fold faster than that of cS_{TT} (Table 2) due to the catalytic contribution of the cleavage-site 2′-OH. Unexpectedly, however, pG binds to $E{\cdot}cS_{rUT}$ with a K_d^{pG} equal to 4500 μM (Table 2), a value significantly greater than both the K_d^{pG} for the binding of pG to the $E{\cdot}cS_{TT}$ complex (730 μM) and the K_d^{pG} for binding of pG to free E [K_d^{pG} = 320 μM (*49*)], suggesting that bound cS_{rUT} somehow interferes with the binding of pG to the ribozyme. Previous experiments have shown that changing the nucleoside at the cleavage site from deoxyribose to ribose has no effect on K_d^{pG} (*49*). However, the following results suggest that the thymidine at position +1 largely causes this effect.

In separate experiments in the background of the all-RNA substrate (CCCUCUAAAAA), we found that replacing the adenosine residue at position +1 with thymidine shifts the K_d^{pG} for binding to the E·S complex from ~10^2 to ~10^4 μM. Removal of the 2′-hydroxyl from position +1 does not cause this ~100-fold effect because K_d^{pG} = 300 μM when S contains 2′-deoxyadenosine at position +1. Although the physical basis remains unclear, this effect, together with the observation that $cS_{T_{mp}T}$ does not affect K_d^{pG}, hint at the possibility that the greater reactivity of the methylene phosphonate monoester substrates ($dS_{T_{mp}T}$ and $cS_{T_{mp}T}$) compared to the corresponding phosphate diester substrates (dS_{TT} and cS_{TT}) results not only from the intrinsically superior reactivity of the modified substrate but also, in part, from a deleterious effect of the thymidine residue at position +1 that is suppressed by the −O− to $-CH_2-$ substitution. It became of interest, therefore, to examine the −O− to $-CH_2-$ substitution in the context of substrates lacking a thymidine residue at position +1 (see below).

Table 3: Comparison of the Guanosine-Independent Endonuclease Reactions of Substrates in the Chimeric DNA−RNA Background[a]

	substrate	$(k_{cat}/K_m)^{S\ b,c}$ ($\times 10^7$ M^{-1} min^{-1})	$k_c(-G)^{b,d}$ (min^{-1})	$k_c(-G)^{rel\ e}$	$K_m(-G)^b$ (nM)	$K_m^{rel\ e}$	$K_{tertiary}(-G)^f$	$K_{tertiary}^{rel\ e}$
cS_{TT}	d(CCC)r(UC)d(TT)rA_4	0.0017	0.0027	(1)	1340	(1)	11	(1)
$cS_{T_{mp}T}$	d(CCC)r(UC)dT_{mp}TrA_4	1.2	0.18	67	152	1/9	130	12

[a] Reactions with ~1 nM 5′-end-labeled substrate, 50 mM NaMES (pH 7.0), and 10 mM $MgCl_2$ at 50 °C. [b] Obtained from nonlinear least-squares fits to plots of k_{obsd} vs [E]. [E] was varied from 0 to 5000 nM. [c] The second-order rate constant for the reaction of E and cS [E + cS → [E•cS]‡ (*28*)]. [d] $k_c(-G)$ is the rate constant for the site specific hydrolysis reaction of substrate with saturating ribozyme in the absence of G and represents the single-turnover reaction E•S → E + P (*28*). [e] $k_c(-G)^{rel}$, K_m^{rel}, and $K_{tertiary}^{rel}$ are values relative to those for cS_{TT}. [f] $K_{tertiary}$ is the equilibrium constant for docking of the P1 duplex into the tertiary interactions with the core of the ribozyme in the absence of G and is calculated from the equation $K_d^S = K^{IGS'}/(1 + K_{tertiary})$ (*4*). It is assumed that $K_m^S = K_d^S$.

Table 4: Comparison of DNA and Chimeric DNA−RNA Substrates Containing a 3′-Terminal Methyl Phosphate or Ethyl Phosphonate

		$(k_{cat}/K_m)^S$ ($\times 10^6$ M^{-1} min^{-1})	k_c (min^{-1})	k_c^{rel}	K_d (nM)	K_d^{rel}
	(i) DNA substrates[a]					
dS_{TOCH_3}	d(C_3UCT)-p-OCH_3	2.43	0.0008	(1)	183	(1)
$dS_{TCH_2CH_3}$	d(C_3UCT)-p-CH_2CH_3	204	0.043	52	126	0.69
	(ii) chimeric substrates[b]					
cS_{TOCH_3}	d(C_3)r(UC)dT-p-OCH_3	110	0.033	(1)	226	(1)
$cS_{TCH_2CH_3}$	d(C_3)r(UC)dT-p-CH_2CH_3	9000	2.26	68	163	0.72

[a] Reactions with 0−2000 nM E, 2.2 mM G, and ~1 nM 5′-end-labeled substrate in 50 mM NaMES (pH 7.0) and 10 mM $MgCl_2$ at 30 °C. [b] Reactions with 10−20000 nM E, 5 mM pG, and ~0.1 nM 5′-end-labeled substrate in 50 mM NaMES (pH 7.0) and 10 mM $MgCl_2$ at 50 °C.

Site Specific Hydrolysis Reaction. In the absence of G, the L-21 *Sca*I ribozyme catalyzes a site specific hydrolysis, albeit much less efficiently than the G-dependent reaction (*28*, *33*). We determined kinetic parameters $(k_{cat}/K_m)^S$, k_c, and K_m directly from plots of k_{obsd} versus E concentration at pH 7.0 (Table 3). The hydrolysis reaction is less well-characterized than the G-dependent reaction; whether $k_c(-G)$ reflects the rate constant for the actual hydrolytic cleavage event and whether $K_m^S(-G)$ equals the equilibrium dissociation constant for dissociation of S from free E remain unclear (*28*). Nevertheless, the ratios of these parameters for $cS_{T_{mp}T}$ and cS_{TT} display strong similarities to the analogous ratios observed in the G-dependent reaction: $cS_{T_{mp}T}$ reacts 67-fold faster than cS_{TT} in the presence of saturating ribozyme (cf. k_c^{rel} in Table 2), and $cS_{T_{mp}T}$ reacts with a K_m value that is 9-fold lower than that of cS_{TT} (cf. K_m^{rel} in Table 3).

Reactions with Substrates Containing 3′-Terminal Methyl Phosphate or Ethyl Phosphonate. The lack of availability of other 5′-deoxy-5′-methylene phosphonate dimers prevented us from examining the bridging −O− to $-CH_2-$ substitution in the context of substrates containing residues other than thymidine at position +1. However, Narlikar et al. (*52*) have shown that the *Tetrahymena* ribozyme efficiently cleaves a substrate containing a 3′-terminal methyl phosphate, in which a methoxy group replaces residues at positions +1 to +5. This observation, coupled with the commercial availability of thymidine methoxyphosphoramidite and thymidine ethylphosphonamidite, raised the possibility of investigating the bridging −O− to $-CH_2-$ substitution in the context of substrates lacking the nucleotidyl moiety following the cleavage site.

The chemical phosphorylation reagent (Glen Research) allows the synthesis of oligonucleotides containing a 3′-terminal phosphate (Scheme 1). When a *P*-methoxyphosphoramidite is used in the coupling cycle that immediately follows installation of the phosphorylation reagent, alkaline workup results in an oligonucleotide containing a 3′-terminal methyl phosphate. By analogy, we anticipated that coupling of a *P*-ethylphosphonamidite after installation of the phosphorylation reagent would result in an oligonucleotide containing a 3′-terminal ethyl phosphonate monoester. To allow comparison with the ribozyme substrates containing the 5′-deoxy-5′-methylenephosphonate thymidine dimer, we synthesized oligonucleotides containing methyl phosphate or ethyl phosphonate termini as both DNA (dS_{TOCH_3} and $dS_{TCH_2CH_3}$) and DNA−RNA chimeric substrates (cS_{TOCH_3} and $cS_{TCH_2CH_3}$) containing ribose residues at U^{-2} and C^{-3}.

We measured the dependence of k_{obsd} for dS_{TOCH_3} and $dS_{TCH_2CH_3}$ on E concentration and determined the kinetic parameters k_c and K_d (Table 4). The results parallel those for the thymidine dimer substrates $dS_{T_{mp}T}$ and dS_{TT}: the phosphonate substrate $dS_{TCH_2CH_3}$ reacts faster than the corresponding control substrate dS_{TOCH_3} and binds in the open complex with nearly the same affinity (K_d = 126 and 183 nM for dS_{TOCH_3} and $dS_{TCH_2CH_3}$, respectively). However, the $-CH_2-$ modification in $dS_{TCH_2CH_3}$ increases k_c by only 52-fold relative to that of dS_{TOCH_3} (Table 4), whereas it increases k_c by ~10^3-fold in the thymidine dimer substrates (Table 1). This difference in relative reactivity arises not from a change in reaction rate of the phosphonate substrate ($dS_{T_{mp}T}$ and $dS_{TCH_2CH_3}$ react with nearly the same k_c values of 0.026 and 0.043 min^{-1}, respectively; Table 4) but from a 44-fold acceleration in the rate of dS_{TOCH_3} relative to that of dS_{TT}. Thus, it appears that changing the nucleotidyl group at positions +1 to +5 (TA_4) to a methyl group has no effect in the context of the bridging $-CH_2-$ group but accelerates the reaction rate by 44-fold in the context of the bridging −O−.

Kinetic characterization of the DNA−RNA chimeric substrates suggests that the $-TA_4$ to $-OCH_3$ modification accelerates the reaction by improving docking of the substrate into the closed complex (Table 4). The ratio of k_c values for $cS_{TCH_2CH_3}$ and cS_{TOCH_3} (k_c^{rel} = 68; Table 4) is the same, within error, as that for the $-TA_4$ substrates (k_c^{rel} = 67; Table 2). However, cS_{TOCH_3} binds to E^G in the closed complex with nearly the same affinity as $cS_{TCH_2CH_3}$, whereas cS_{TT} binds

Table 5: Effect of Oxygen to Methylene Substitution in Nonenzymatic Reactions of Phosphate Esters[a]

	k_2 ($\times 10^5$ M^{-1} min^{-1})		
nucleophile	phosphate (MNP)	methylene phosphonate (ENP)	elemental effect $k(CH_2)/k(O)$
hydroxide[b]	6.6 (4.6)[e]	31.9	4.8
ethanolamine[c]	0.3	1.0	3.0
hydroxylamine[d]	3.5	18.2	5.2

[a] Reactions at 25 °C. [b] Ionic strength of 1.7 (KCl); determined from five reactions with 0.3−1.7 M potassium hydroxide and 0.1 mM MNP or ENP. [c] Ionic strength of 2.0 (KCl); determined from five reactions with 0.1−2.0 M ethanolamine hydrochloride as buffer (pH 9.7) and 0.1 mM MNP or ENP. [d] Ionic strength of 2.0 (KCl); determined from five reactions with 0.1−2.0 M hydroxylamine hydrochloride as buffer (pH 6.0) and 10 mM MNP or ENP. [e] Determined by NMR. Ionic strength of 1.7 (KCl); determined from five reactions with 0.3−1.7 M potassium hydroxide and 10 mM MNP.

to E^G in the closed complex with nearly 10-fold lower affinity than $cS_{T_{mp}T}$. These results indicate that in the context of substrates containing a 5′-bridging oxygen, the ribozyme is sensitive to the moiety following the cleavage site during the docking step, and that methylene substitution appears to suppress this discrimination.

Intrinsic Reactivity Difference between a Phosphate Diester and a Phosphonate Monoester: Reactions of Methyl 4-Nitrophenyl Phosphate (MNP) and Ethyl 4-Nitrophenyl Phosphonate (ENP) with Nucleophiles. MNP was synthesized as described by Ba-Saif et al. (*57*). ENP had not been synthesized previously, but Kelly synthesized several aryl phosphonate monoesters by reaction of the appropriate phosphonic acid dichloride in the presence of an excess of the appropriate phenol and DMF, followed by hydrolytic workup (*58*). DMF reportedly prevents formation of the phosphonate diester (*58*). However, we found that ethylphosphonic acid dichloride reacts with 4-nitrophenol to form the diester, bis(4-nitrophenyl)ethylphosphonate, even in the presence of DMF. To obtain the desired ENP monoester, therefore, we had to isolate the diester and subject it to alkaline hydrolysis (see the Supporting Information).

The second-order rate constants for reactions of various nucleophiles with the phosphorus centers of MNP and ENP at the same ionic strength were determined spectrophotometrically (Scheme 2 and Table 5). Hydroxide reacts with MNP with the same second-order rate constant (within 10%) as that reported by Rahil and Pratt (5.8×10^5 M^{-1} min^{-1}) (*32*). We obtained the same value (within 30%) when we monitored this reaction by ^{1}H NMR (see Materials and Methods). ENP reacts faster than MNP in reactions with hydroxide, ethanolamine, and hydroxylamine by factors of 4.8, 3.0, and 5.2, respectively.

DISCUSSION

Overall Kinetic and Thermodynamic Effects of Replacing the 5′-Bridging Oxygen of the Reactive Phosphoryl Group with a Methylene Group in the Ribozyme-Catalyzed Phosphoryl Transfer Reaction. We synthesized oligonucleotide substrates containing thymidines flanking the reactive phosphoryl group and quantitatively investigated the effect of a 5′-O to 5′-CH_2 modification on both ground state binding and transition state stabilization. In the context of a substrate containing only deoxyribose residues, the CH_2 modification increases the rate of the endonuclease reaction by (1.4×10^3)-fold over that for the corresponding unmodified substrate, thereby providing 4.4 kcal mol^{-1} of transition state stabilization. This surprising difference in reactivity does not arise from differences in base-pairing affinities of the substrates for the IGS of the ribozyme; it arises from differences in the reactivity of the E^G•S ternary complex (k_c). Since k_c for DNA substrates includes both the docking of the substrate helix into the catalytic core and the actual chemical step (see Figure 2), it was not possible to attribute the favorable effect of the $-CH_2-$ group to the docking step or to the actual chemical cleavage step.

To distinguish effects on docking from effects on chemistry, we analyzed the 5′-O to 5′-CH_2 modification in the context of DNA−RNA chimeric substrates containing 2′-hydroxyl groups at positions C^{-2} and U^{-3}. These 2′-hydroxyl groups make tertiary interactions with the ribozyme core that stabilize docking of the substrate in the ground state, thereby providing a means for probing the docking step and the chemical step independently (*4*, *31*, *36*, *38*−*47*). In the chimeric background, the methylene substrate $cS_{T_{mp}T}$ binds to the ribozyme ∼10-fold more tightly and reacts in the E^G•S ternary complex ∼70-fold faster than does the unmodified substrate, cS_{TT}. As both substrates bind to the IGS analogue, IGS′, with very similar affinities, we attribute the tighter binding of $cS_{T_{mp}T}$ to formation of stronger tertiary interactions. Thus, the $\sim 10^3$-fold stimulation of DNA cleavage upon 5′-O to 5′-CH_2 substitution arises from an ∼10-fold effect on docking and an $\sim 10^2$-fold effect on chemistry. Below, we discuss the possible factors that could contribute to these effects.

In the course of our experiments, we discovered that the thymidine residue at position +1 of S dramatically weakens the binding of G to the ES complex. For the "wild-type" RNA substrate rCCCUCUA^{+1}AAAA, pG binds to the ES complex with a K_d^{pG} equal to 100 μM, similar to the value reported previously (*49*). However, pG binds to the ES complexes of r(CCCUCU)dTr(AAAA) and d(CCC)r(UCU)-dTr(AAAA) with K_d^{pG} values equal to 10 000 and 4500 μM, respectively. The physical basis of this effect, though not understood, may provide an additional strategy by which the *Tetrahymena* group I intron ensures the fidelity of 5′-splice site cleavage during self-splicing; splice sites lacking the correct +1 nucleotide might undergo splicing more slowly than those containing it because of weaker G binding at the active site. Whether this effect is specific to thymidine substitution and whether it is unique to the *Tetrahymena* ribozyme or reflects a general strategy used by other group I introns to enhance 5′-splice site cleavage fidelity remains to be determined. With respect to the current investigation, however, the anomalous effects from the +1 T substitution together with the smaller values of K_d^{pG} and K_d^S for the reaction of $cS_{T_{mp}T}$ as compared to those for the reaction of cS_{TT} (Table 2) raised concern that the effect of the 5′-O to $-CH_2-$ substitution could be context-dependent; i.e., the significantly greater reactivity of the methylene phosphonate substrate might reflect partially the ability of the methylene group to suppress inherently deleterious effects of the thymidine at position +1. For this reason, we studied the $-O-$ to $-CH_2-$ modification in the context of substrates lacking the thymidine at position +1.

Using the chemical phosphorylation reagent together with thymidine *p*-methoxyphosphoramidite or thymidine *p*-ethylphosphonamidite, we prepared substrates containing a 3′-terminal methylphosphoryl group (dS_{TOCH_3} and cS_{TOCH_3}) or an ethylphosphonyl group ($dS_{TCH_2CH_3}$ and $cS_{TCH_2CH_3}$) at the scissile phosphorus center. The phosphonate monoester substrates, $dS_{TCH_2CH_3}$ and $cS_{TCH_2CH_3}$, bind and react with nearly the same K_d^s and k_c values as $dS_{T_{mp}T}$ and $cS_{T_{mp}T}$, respectively (Table 4), showing no effect from removal of the $-TA_4$ nucleotidyl group. The normal phosphodiester substrates, on the other hand, do show a dependence on the 3′-terminal moiety. The DNA−RNA chimeric substrates (cS_{TOCH_3} and cS_{TT}) react with similar k_c values, but cS_{TOCH_3} binds more tightly to the ribozyme than cS_{TT} does, suggesting that replacing the $-TA_4$ nucleotidyl group with a methoxy group allows better docking of the substrate into the catalytic core. The phosphate diester substrate, cS_{TOCH_3}, binds to the ribozyme with nearly the same affinity as the phosphonate monoester, $cS_{TCH_2CH_3}$.

Importantly, the ratio of k_c values for $cS_{TCH_2CH_3}$ and cS_{TOCH_3} ($k_c^{rel} = 68$) is the same as that for cS_{TmpT} and cS_{TT} ($k_c^{rel} = 67$), suggesting that the effect of the $-CH_2-$ modification on the actual chemical step is context-independent. For the DNA substrates, replacing the $-TA_4$ nucleotidyl group with a methoxy group stimulates reactivity by ~44-fold, possibly reflecting the enhanced docking of dS_{TOCH_3} relative to dS_{TT}, as in the case of the chimeric substrates. Presumably, this enhanced docking of the 3′-terminal methyl phosphate substrate eliminates differences in docking that may occur between dS_{TT} and $dS_{T_{mp}T}$ as the phosphonate monoester ($dS_{TCH_2CH_3}$) reacts only 52-fold faster than the phosphate diester (dS_{TOCH_3}). This ratio of k_c values is similar to the ratio of k_c values observed for the DNA−RNA chimeric substrates (67−68-fold) and further suggests that the observed k_c^{rel} values are context-independent and are intrinsic to the ribozyme reaction.

Reactivity of a Phosphonate Monoester and a Phosphate Diester in Nonenzymatic Reactions with Nucleophiles. We addressed whether the ~10^2-fold stimulatory effect of the $-CH_2-$ modification on the rate constant for chemical cleavage (k_c) could arise from a difference in the intrinsic reactivity of a phosphonate monoester versus a phosphate diester toward nucleophiles. Although numerous comparisons of the reactivity of phosphonates versus phosphates have been described, there are contradictory reports in the literature about their relative reactivity. Harris et al. (*59*) found that uridine 2′,3′-cyclic phosphonate reacts with hydroxide ~4-fold *slower* than the corresponding 2′,3′-cyclic phosphate. However, the sensitivity of cyclic ester reactions to geometric factors (*60*) casts doubt on the relevance of this result to the acyclic substrates used herein, as the changes in bond lengths and angles that arise from the $-CH_2-$ substitution could influence the relative reactivity of the cyclic and acyclic esters differently.

In another report, Tsubouchi and Bruice (*61*) proposed that methyl phosphonate monoesters would undergo alkaline hydrolysis at a rate *similar* to that of phosphate diesters when the leaving groups are the same. On this basis, they estimated the rate of hydrolysis of methyl phosphonates using the previously established relationship between the bimolecular rate of OH^--catalyzed phosphate diester hydrolysis (k_{OH^-}) and the leaving group pK_a (*62*):

$$\log k_{OH^-} = 0.69 - 0.76 pK_a \quad (4)$$

Using eq 4, they calculated the k_{OH^-} values for hydrolysis of phenyl methyl phosphonate and *p*-nitrophenyl methyl phosphonate to be 1.8×10^{-7} and 1.8×10^{-5} M^{-1} s^{-1}, respectively (*61*). In support of their proposal, these calculated values are reasonably close to the experimental values of 5.6×10^{-7} and 5.0×10^{-5} M^{-1} s^{-1} (*63*), respectively.

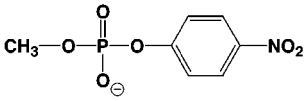

p-nitrophenyl methyl phosphate

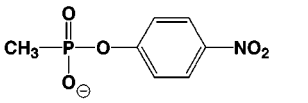

p-nitrophenyl methyl phosphonate

In another comparison, Rahil and Pratt argued that phosphonates should react *considerably faster* than analogous phosphates in reactions with nucleophiles (*32*, *64*−*66*). They directly compared the alkaline hydrolysis rates of *p*-nitrophenyl methyl phosphate and *p*-nitrophenyl methyl phosphonate and found that the phosphonate monoester reacted ~29-fold faster than the diester. Unfortunately, the compounds used by Rahil and Pratt were not isostructural, so the observed ~29-fold difference in reactivity need not reflect exclusively the elemental effect of $-O-$ to $-CH_2-$ substitution.

To obtain an estimate of the intrinsic reactivity effects caused by the $-O-$ to $-CH_2-$ substitution, we compared the reactivity of a phosphate diester with that of the corresponding *isostructural* phosphonate monoester. *p*-Nitrophenyl methyl phosphate (MNP) and *p*-nitrophenyl ethyl phosphonate (ENP) were synthesized, and their reactivities with both oxygen and nitrogen nucleophiles were measured under the same conditions (see Table 5). In contrast to the results of Rahil and Pratt (*32*), we found that with each nucleophile the phosphonate monoester reacts *modestly faster* (3−5-fold) than the phosphate diester.

Accounting for the Stimulatory Effect of the $-CH_2-$ Modification on the Ribozyme Reaction. If it is assumed that the relative reactivity of MNP and ENP reflects that of the substrates used herein,[2] the ~5-fold difference in intrinsic chemistry does not account fully for the ~10^2-fold stimulatory effect of the 5′-O to 5′-CH_2 substitution observed in the ribozyme-catalyzed cleavage reactions. Possibly, the ribozyme active site better accommodates a phosphonate transition state; that is, the ribozyme binds a transition state containing an equatorial methylene group more tightly (relative to the ground state) than it binds a transition state containing an equatorial oxygen atom (relative to the ground state). The geometric and chemical effects of the 5′-O to 5′-CH_2 substitution suggest possible factors that could contribute to differential transition state stabilization. X-ray crystallographic data for the related compounds, 2-aminoethyl phosphate (*67*, *68*) and 2-aminoethyl phosphonic acid (*69*), reveal the following differences: (1) the P−C bond is

[2] In using MNP and ENP as model compounds for the relative reactivity of nucleotidyl phosphate diesters and phosphonate monoesters, respectively, there is an inherent assumption that the nucleotidyl esters exhibit the same reaction profile as the model compounds even though the leaving groups are different (*p*-nitrophenoxide vs nucleotidyl 3′-alkoxide).

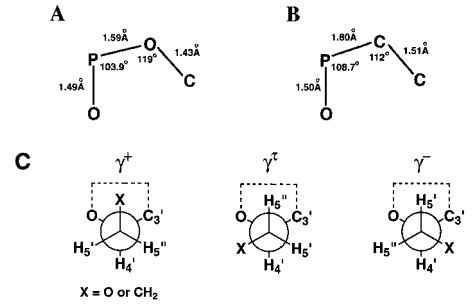

FIGURE 5: Geometric comparison of a phosphate (A) and its isosteric phosphonate counterpart (B). Data are from the crystallographic structure of 2-aminoethyl phosphate (*67*, *68*) and 2-aminoethyl phosphonic acid (*69*). (C) Staggered rotamers around the C4′−C5′ nucleoside bond [adapted from Szabo (*70*)].

considerably longer (by 0.21 Å) than the corresponding P−O bond, (2) the angle ∠CPO is modestly larger (by 4.8°) than ∠OPO (Figure 5A,B), and (3) the phosphonate center occupies a greater molecular volume than the phosphate center. Additionally, NMR data show that the $-CH_2-$ modification introduces a change in the distribution of rotamers about the C4′−C5′ axis (γ) [Figure 5C (*70*)]. Whereas natural nucleotides have a marked preference for the γ^+ rotamer, a 5′-deoxy-5′-methylphosphonate-linked thymidine dimer populates the γ^t and γ^- rotamers. Together, these factors could provide a slightly different spatial arrangement of functional groups that the active site better accommodates.

Further differences between the phosphonate monoester and the phosphate diester could arise in the transition state depending on the relative extents of bonding to the leaving group and the nucleophile. However, the nonenzymatic reactions of phosphonate monoesters with nucleophiles appear to occur by the same reaction pathway and transition state structure as those of phosphate diesters with nucleophiles. Both types of reactions show the hallmarks of an S_N2 P mechanism: a linear dependence of reaction rate on nucleophile concentration and a similar sensitivity of the reaction rate to steric[3] and electronic[4] features of the nucleophile (*1*−*3*, *63*, *71*). The reactions of the two esters also display similar sensitivities to the pK_a's of the nucleophiles and leaving groups (*1*, *2*). For the reactions of *p*-nitrophenyl methyl phosphonate with substituted pyridines, plots of the logarithm of the second-order rate constant versus the pK_a of the pyridine gave a slope (β_{nuc}) of 0.29 (reactions at 60 °C; pK_a values at 60 °C) (*1*), a value similar to the value of 0.31 obtained for the reactions of substituted pyridines with 2,4-dintirophenyl methyl phosphate (reactions at 39 °C with 1 M KCl) (*1*, *2*). Although β_{lg} has not been determined directly for the phosphonate analogue, the change in the relative rate observed for *p*-nitrophenyl methyl phosphonate and phenyl methyl phosphonate with hydroxide [$k^{rel} = 89$ (*63*)] is similar to that predicted for the corresponding phosphate diesters by eq 4 ($k^{rel} = 134$), suggesting that β_{lg} is similar for the phosphonate monoester and the phosphate diester in reactions with hydroxide. The similarities in β_{nuc} and β_{lg} indicated here suggest that the changes in charge that occur on the nucleophile and the leaving group as the phosphonate monoester transition state forms are similar to those that occur as the phosphate diester transition state forms. Although these data imply strong similarities between the two transition states, even very slight changes in transition state structure can result in significant effects on catalytic efficiency.

An alternative explanation for the differential transition state stabilization pertains to the difference in hydrophobicity between the $-O-$ and $-CH_2-$ groups, whereby the active site desolvates the 5′-position in the transition state and consequently favors the reaction of the phosphonate monoester over the phosphate diester. We can estimate the magnitude of transition state stabilization that might arise from such a hydrophobic effect using data for the partitioning of a methylene ($-CH_2-$) and ether oxygen ($-O-$) between water and octanol. The free energy cost at 50 °C for transferring an $-O-$ from water to octanol relative to $-CH_2-$ [$\Delta\Delta G_{tr}(-O-/-CH_2-)$] is 2.2 kcal mol^{-1} (*72*), large enough to account entirely for the observed differences in transition state stabilization between the phosphonate monoester and the phosphate diester reaction. However, the partitioning of an ether oxygen between water and octanol may not represent accurately that for a phosphate ester oxygen. In fact, the bridging oxygen atom of a phosphate ester is electropositive relative to the oxygen atom of an ether due to $p_\pi-d_\pi$ bonding interactions in which the lone pair electrons on oxygen delocalize into the phosphorus center (*73*). Linear free energy relationships indicate that the effective charge (ϵ) on the bridging oxygen of a phosphate diester ($\epsilon \cong 0.7$) (*73*) resembles more closely the effective charge on the bridging oxygen of a carboxylate ester ($\epsilon \cong 0.7$) (*74*, *75*) rather than that of an ether oxygen ($\epsilon \cong 0$) (*75*). Consequently, comparison of ΔG_{tr}(water→octanol) for the carboxylate ester, methyl acetate, and the corresponding isostructural ketone, 2-butanone, may reflect more accurately the hydrophobic effect of the 5′-O to CH_2 substitution at a phosphoester center. Using a ΔG_{tr}(water→octanol) for methyl acetate of −0.3 kcal mol^{-1} (*72*) and a ΔG_{tr}(water→octanol) for butanone of −0.4 kcal mol^{-1} (*72*), we obtain a $\Delta\Delta G_{tr}(-O-/-CH_2-)$ of ∼0.1 kcal mol^{-1}. Therefore, even if a change in solvation occurs in the chemical step that resembles the transfer of the 5′-atom from water to a hydrophobic solvent, the hydrophobic effect appears to be unable to account for the greater transition state stabilization of the phosphonate monoester relative to the phosphate diester. The small value of $\Delta\Delta G_{tr}(-O-/-CH_2-)$ would increase if electron density accumulated on the bridging oxygen atom during the reaction. However, arguments below suggest that the bridging oxygen of the transferred phosphoryl group undergoes only a slight decrease in electropositive character in the transition state.

Transition State Interactions with the Bridging Oxygen Atom of the Transferred Phosphoryl Group Provide Little Catalytic Advantage to Phosphoryl Transferases. Because the methylene group can neither accept or donate a hydrogen bond nor coordinate a metal ion, the observation that 5′-methylene substitution does not have a deleterious effect on the ribozyme reaction suggests the absence of important interactions with the 5′-oxygen in the transition state. The following arguments suggest that during nucleophilic dis-

[3] The sterically hindered nucleophile 2-picoline reacts more than 100-fold slower than the unhindered nucleophile (3-picoline) possessing the same pK_a (*1*, *2*).

[4] Both reactions display the α effect whereby hydroperoxide anion reacts more than 100-fold faster than hydroxide anion despite having a pK_a almost 4 units lower than hydroxide (*1*, *2*).

placement reactions of phosphate diesters the electron density on the bridging oxygen atom of the transferred phosphoryl group (O_{tg}) changes modestly. Consequently, interactions with O_{tg} such as H-bonding or metal ion coordination should not be strengthened significantly in the transition state and therefore would provide little catalytic advantage to phosphoryl transferase enzymes.

For the reaction of a phosphate diester with a nucleophile, relating the logarithm of a reaction rate constant (log k_{obsd}) to the pK_a of the leaving group gives a linear free energy relationship with the slope β_{lg} that provides information about the buildup of negative charge on the leaving group in the transition state (*75*, *76*). Analogously, the dependence of log k_{obsd} on the pK_a of the transferred group (β_{tg}) provides information about the buildup of negative charge on O_{tg} in the transition state. To the best of our knowledge, however, β_{tg} has never been determined for the reactions of phosphate diesters with nucleophiles.

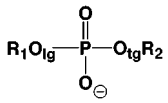

Chin et al. studied the reaction of hydroxide with a series of phosphate diesters in which the substituents on both esterified oxygens (the leaving group and the transferred group) were varied simultaneously and equivalently (i.e., $R_1 = R_2$) (*62*). To a first approximation, the observed sensitivity of the reaction rate to a change in substituent relative to the pK_a of ROH reflects the sum of the effects from changing both the leaving group and the transferred group:

$$\beta_{obsd} = \beta_{lg} + \beta_{tg} \quad (5)$$

The value of β_{obsd} (-0.76) obtained by Chin et al. therefore approximates roughly the effective charge changes experienced by the esterified oxygen atoms together in going from the ground state to the transition state. Analogously, Kirby and Younas determined the rate constants (k_{OH^-}) for the reaction of hydroxide with a series of bis(aryl)phosphate diesters (*3*) in which both the leaving group and the transferred group contained the same aryl group ($R_1 = R_2$). We plotted the logarithm of these reported rate constants versus the pK_a of the corresponding phenols and obtained a β_{obsd} of approximately -0.8,[5] a value similar to that reported by Chin et al. To obtain a measure of β_{lg} alone, we (C. D. Barth, P. S. R. Anjaneyulu, and J. A. Piccirilli, unpublished results) measured k_{OH^-} for a series of methyl aryl phosphate diesters in which the substituent on the leaving group was varied while the substituent on the transferred group remained the same. This analysis gave a β_{lg} of approximately -0.7, which via eq 5 gives a β_{tg} of approximately -0.1. In reactions with hydroxide then, the effective charge (ϵ) on the bridging oxygen atom of the phosphate diester changes only from 0.7 in the ground state to 0.6 in the transition state. The data of Hengge et al. (*77*) suggest that β_{tg} may be even smaller than -0.1. *p-tert*-Butylphenyl *p*-nitrophenyl phosphate reacts with hydroxide at pH 13 only 4-fold faster than 3,3-dimethylbutyl *p*-nitrophenyl phosphate reacts under the same conditions (*77*), even though the *tert*-butylphenoxy group should be considerably more electron withdrawing (p$K_a = 10$) than the 3,3-dimethylbutyloxy group (p$K_a = 16$). A two-point Bronstead plot gives a β_{tg} of approximately -0.01, confirming that β_{tg} is small. This small change in effective charge means that O_{tg} remains electropositive (relative to the oxygen of H_2O) throughout the reaction and therefore possesses little potential for transition state stabilization via metal ion coordination[6] or hydrogen bonding.[7]

In conclusion, a physical organic description of the effective charge change on O_{tg} during phosphoryl transfer suggests that enzymes generally will gain little catalytic advantage from interactions (metal ion or H-bond) with the bridging oxygen of the transferred phosphoryl group. However, an active site could mediate a network of highly cooperative interactions that would involve O_{tg} such that disruption of this inherently weak interaction could also disrupt other energetically important interactions. This does not seem to be the case for the *Tetrahymena* ribozyme, however, as the methylene modification does not disrupt catalysis.

Phosphonate Monoesters as Biochemical Probes. Methylene phosphonate monoesters possess structure, electronic, and reactivity properties that closely mimic those of natural phosphate diesters and therefore may provide valuable tools with which to explore the mechanism of phosphoryl transferase enzymes as described herein. Additionally, phosphonate monoesters may complement phosphorothioates as probes for determining whether the chemical step limits the rate of an enzyme-catalyzed process. Phosphorothioate diesters react modestly slower than normal phosphate diesters in nonenzymatic reactions with nucleophiles (*33*); a similarly modest inhibitory effect on an enzyme-catalyzed reaction provides evidence that the chemical step limits the enzyme-catalyzed reaction rate (*33*). Analogously, as methylene

[5] We plotted the logarithm of the rate constants for the reactions of hydroxide with bis-2,4-dinitrophenyl phosphate ($k_{OH^-} = 1.51 \times 10^{-1}$ min^{-1}), bis-4-nitrophenyl phosphate ($k_{OH^-} = 5.62 \times 10^{-4}$ min^{-1}), and bis-3-nitrophenyl phosphate ($k_{OH^-} = 4.89 \times 10^{-5}$ min^{-1}) versus the pK_a's of 2,4-dinitrophenol (4.07), bis-4-nitrophenyl phosphate (7.15), and bis-3-nitrophenyl phosphate (8.35), respectively. Values for rate constants were from Kirby and Younas (*3*). The resulting linear free energy relationship gave a slope (β_{obsd}) of -0.82 (correlation coefficient = 1).

[6] The analysis of Narlikar et al. suggested that a change in effective charge of -1 on an oxygen atom results in a change in Mg^{2+} affinity for that oxygen atom of ($\sim 3.2 \times 10^3$)-fold (*4*). Thus, if the effective charge on O_{tg} increases in the transition state by -0.1, the Mg^{2+} binding affinity would increase by only 2.2-fold $\{\exp[0.1 \times \ln(3.2 \times 10^3)]\}$, reflecting little potential for transition state stabilization.

[7] We can estimate the potential contribution that a hydrogen bond to O_{tg} could make to transition state stabilization by first relating the effective charge change on O_{tg} to the change in its pK_a (ΔpK_a) followed by relating ΔpK_a to the change in H-bond strength. The effective charges on the oxygen atoms of ROH and RO^- are 0 and -1, respectively. As the pK_a's of ROH and RO^- are -1.7 and 16, respectively, a change in effective charge of -1 corresponds to a ΔpK_a of 17.7. If the effective charge on O_{tg} changes maximally from 0.7 to 0.6 on going from the ground state to the transition state, its pK_a changes by 1.8 units. Shan et al. (*5*) investigated the change in hydrogen bond strength K^{HB} as a function of ΔpK_a for an intramolecular H-bond in a series of substituted salicylate monoanions. The dependence of log K^{HB} upon ΔpK_a was linear, but steeper in dimethyl sulfoxide ($\beta = 0.73$) than in water ($\beta = 0.05$), revealing a greater strengthening of the H-bond with changes in the pK_a values of the donor or acceptor in DMSO than in water (*5*). If this dependence on H-bond strength in water and DMSO were to hold for the solution and ribozyme active site H-bonds, respectively, an H-bond interaction with O_{tg} would be expected to provide a maximum rate enhancement of only 17-fold (Δp$K_a \cong 1.8$; rate enhancement = $10^{\Delta pK_a \Delta\beta} = 10^{1.8\cdot(0.73-0.05)}$; $\Delta\Delta G^{\ddagger} \cong 1.8$ kcal/mol).

phosphonate monoesters react modestly faster than phosphate diesters in nonenzymatic reactions with nucleophiles, a similarly modest stimulatory effect on the enzymatic reaction also would imply rate-limiting chemistry. The geometric and chemical changes caused by sulfur substitution often can inhibit enzymatic reactions for reasons other than the "intrinsic" chemical effect of the modification (*33* and references therein). Additionally, phosphoryl transferases often mediate catalysis via interactions with the nonbridging phosphoryl oxygen atoms such that phosphorothioates exhibit strongly deleterious effects, thereby precluding their utility as mechanistic probes. In contrast, the geometric and chemical changes rendered by the 5′-methylene substitution appear to be more subtle and less likely to exhibit strongly deleterious effects on an enzymatic reaction. For these reasons, the phosphonate monoester ultimately may prove to be more advantageous than the phosphorothioate as a probe for the rate-limiting step.

Summary. Much of the work on phosphoryl transferase enzymes exploits atomic mutagenesis in probing the interactions between the enzyme and substrate(s). Almost always, this work has focused on the leaving group, the nonbridging phosphoryl oxygen atoms, and other atoms near the reaction center, but not on the bridging oxygen atom of the transferred phosphoryl group (O_{tg}). Here we addressed in a quantitative way the effect of changing this oxygen atom to a $-CH_2-$ group in the *Tetrahymena* ribozyme reaction. We found that substrates containing this modification react substantially faster ($\sim 10^2$-fold) than the natural phosphate diester linkage. To calibrate this effect, we measured the relative reactivity of a model phosphonate monoester and its isostructural phosphodiester counterpart in nonenzymatic reactions with nucleophiles and found that the phosphonate reacted only modestly faster ($\sim$5-fold). The greater stimulatory effect of the $-CH_2-$ modification in the ribozyme reaction compared to the nonenzymatic reaction may arise fortuitously from the change in molecular geometry engendered by the modification. More importantly, however, these results show that the lack of H-bonding or metal ion coordination capability at the 5′-position has no adverse effect on the ribozyme reaction, strongly suggesting the absence of such interactions during group I intron splicing. Even if such interactions did occur, so little charge builds up on the 5′-oxygen during the reaction that they would provide little catalytic advantage.

ACKNOWLEDGMENT

We thank Margarita Chlopecki for excellent technical assistance, and members of the Piccirilli lab for helpful discussion and critical comments on the manuscript.

SUPPORTING INFORMATION AVAILABLE

Synthesis and characterization of ethyl 4-nitrophenyl phosphonate (ENP) and methyl 4-nitrophenyl phosphate (MNP). This material is available free of charge via the Internet at http://pubs.acs.org.

REFERENCES

1. Brass, H. J., Edwards, J. O., and Biallas, M. J. (1970) *J. Am. Chem. Soc. 92*, 4675−4681.
2. Kirby, A. J., and Younas, M. (1970) *J. Chem. Soc. B*, 1165−1172.
3. Kirby, A. J., and Younas, M. (1970) *J. Chem. Soc. B*, 510−513.
4. Narlikar, G. J., Khosla, M., Usman, N., and Herschlag, D. (1997) *Biochemistry 36*, 2465−2477.
5. Shan, S. O., and Herschlag, D. (1996) *Proc. Natl. Acad. Sci. U.S.A. 93*, 14474−14479.
6. Shan, S. O., Kravchuk, A. V., Piccirilli, J. A., and Herschlag, D. (2001) *Biochemistry 40*, 5161−5171.
7. Shan, S. O., Yoshida, A., Sun, S., Piccirilli, J. A., and Herschlag, D. (1999) *Proc. Natl. Acad. Sci. U.S.A. 96*, 12299−12304.
8. Piccirilli, J. A., Vyle, J. S., Caruthers, M. H., and Cech, T. R. (1993) *Nature 361*, 85−88.
9. Weinstein, L. B., Jones, B. C. N. M., Cosstick, R., and Cech, T. R. (1997) *Nature 388*, 805−808.
10. Sjogren, A. S., Pettersson, E., Sjoberg, B. M., and Stromberg, R. (1997) *Nucleic Acids Res. 25*, 648−653.
11. Yoshida, A., Sun, S., and Piccirilli, J. A. (1999) *Nat. Struct. Biol. 6*, 318−321.
12. Strobel, S. A., and Ortoleva-Donnelly, L. (1999) *Chem. Biol. 6*, 153−165.
13. Herschlag, D., and Khosla, M. (1994) *Biochemistry 33*, 5291−5297.
14. Yoshida, A., Shan, S. O., Herschlag, D., and Piccirilli, J. A. (2000) *Chem. Biol. 7*, 85−96.
15. Engel, R. (1977) *Chem. Rev. 77*, 349−367.
16. Miller, P. S., Reddy, M. P., Murakami, A., Blake, K. R., Lin, S. B., and Agris, C. H. (1986) *Biochemistry 25*, 5092−5097.
17. Miller, P. S., McParland, K. B., Jayaraman, K., and Ts'o, P. O. (1981) *Biochemistry 20*, 1874−1880.
18. Disney, M. D., Testa, S. M., and Turner, D. H. (2000) *Biochemistry 39*, 6991−7000.
19. Labeots, L. A., and Weiss, M. A. (1997) *J. Mol. Biol. 269*, 113−128.
20. Miller, P. S., Yano, J., Yano, E., Carroll, C., Jayaraman, K., and Ts'o, P. O. (1979) *Biochemistry 18*, 5134−5143.
21. Noble, S. A., Fisher, E. F., and Caruthers, M. H. (1984) *Nucleic Acids Res. 12*, 3387−3404.
22. Boehringer, M. P., Graff, D., and Caruthers, M. H. (1993) *Tetrahedron Lett. 34*, 2723−2726.
23. Szabo, T., Kers, A., and Stawinski, J. (1995) *Nucleic Acids Res. 23*, 893−900.
24. Heinemann, U., Rudolph, L. N., Alings, C., Morr, M., Heikens, W., Frank, R., and Blocker, H. (1991) *Nucleic Acids Res. 19*, 427−433.
25. Arni, R. K., Watanabe, L., Ward, R. J., Kreitman, R. J., Kumar, K., and Walz, F. G. (1999) *Biochemistry 38*, 2452−2461.
26. Breaker, R. R., Gough, G. R., and Gilham, P. T. (1993) *Biochemistry 32*, 9125−9128.
27. Zaug, A. J., Grosshans, C. A., and Cech, T. R. (1988) *Biochemistry 27*, 8924−8931.
28. Herschlag, D., and Cech, T. R. (1990) *Biochemistry 29*, 10172−10180.
29. Herschlag, D., and Cech, T. R. (1990) *Biochemistry 29*, 10159−10171.
30. Herschlag, D., and Cech, T. R. (1990) *Nature 344*, 405−409.
31. Knitt, D. S., Narlikar, G. J., and Herschlag, D. (1994) *Biochemistry 33*, 13864−13879.
32. Rahil, J., and Pratt, R. F. (1993) *Biochem. J. 296*, 389−393.
33. Herschlag, D., Piccirilli, J. A., and Cech, T. R. (1991) *Biochemistry 30*, 4844−4854.
34. Robertson, D. L., and Joyce, G. F. (1990) *Nature 344*, 467−468.
35. Zaug, A. J., and Cech, T. R. (1986) *Science 231*, 470−475.
36. Bevilacqua, P. C., Kierzek, R., Johnson, K. A., and Turner, D. H. (1992) *Science 258*, 1355−1358.
37. Bevilacqua, P. C., Li, Y., and Turner, D. H. (1994) *Biochemistry 33*, 11340−11348.
38. Herschlag, D. (1992) *Biochemistry 31*, 1386−1399.
39. Herschlag, D., Eckstein, F., and Cech, T. R. (1993) *Biochemistry 32*, 8299−8311.
40. Pyle, A. M., and Cech, T. R. (1991) *Nature 350*, 628−631.
41. Pyle, A. M., Moran, S., Strobel, S. A., Chapman, T., Turner, D. H., and Cech, T. R. (1994) *Biochemistry 33*, 13856−13863.

42. Pyle, A. M., Murphy, F. L., and Cech, T. R. (1992) *Nature 358*, 123−128.
43. Strobel, S. A., and Cech, T. R. (1993) *Biochemistry 32*, 13593−13604.
44. Strobel, S. A., and Cech, T. R. (1995) *Science 267*, 675−679.
45. Sugimoto, N., Sasaki, M., Kierzek, R., and Turner, D. H. (1989) *Chem. Lett.*, 2223−2226.
46. Wang, J.-F., and Cech, T. R. (1994) *J. Am. Chem. Soc. 116*, 4178−4182.
47. Wang, J. F., Downs, W. D., and Cech, T. R. (1993) *Science 260*, 504−508.
48. Li, Y., and Turner, D. H. (1997) *Biochemistry 36*, 11131−11139.
49. McConnell, T. S., Cech, T. R., and Herschlag, D. (1993) *Proc. Natl. Acad. Sci. U.S.A. 90*, 8362−8366.
50. Profenno, L. A., Kierzek, R., Testa, S. M., and Turner, D. H. (1997) *Biochemistry 36*, 12477−12485.
51. Narlikar, G. J., Bartley, L. E., Khosla, M., and Herschlag, D. (1999) *Biochemistry 38*, 14192−14204.
52. Narlikar, G. J., Gopalakrishnan, V., McConnell, T. S., Usman, N., and Herschlag, D. (1995) *Proc. Natl. Acad. Sci. U.S.A. 92*, 3668−3672.
53. Narlikar, G. J., and Herschlag, D. (1998) *Biochemistry 37*, 9902−9911.
54. Narlikar, G. J., and Herschlag, D. (1996) *Nat. Struct. Biol. 3*, 701−710.
55. Herschlag, D., Eckstein, F., and Cech, T. R. (1993) *Biochemistry 32*, 8312−8321.
56. Knitt, D. S., and Herschlag, D. (1996) *Biochemistry 35*, 1560−1570.
57. Ba-Saif, S. A., Davis, A. M., and Williams, A. (1989) *J. Org. Chem. 54*, 5483−5486.
58. Kelly, S. J. S. (1974) The synthesis and enzymic hydrolysis of phosphonate monoesters, organophosphorous analogs of phosphate esters. 101 pp, Ph.D. thesis (11−23).
59. Harris, M. R., Usher, D. A., Albrecht, H. P., Jones, G. H., and Moffatt, J. G. (1969) *Proc. Natl. Acad. Sci. U.S.A. 63*, 246−252.
60. Westheimer, F. H. (1968) *Acc. Chem. Res. 1*, 70−78.
61. Tsubouchi, A., and Bruice, T. C. (1995) *J. Am. Chem. Soc. 117*, 7399−7411.
62. Chin, J., Banaszczyk, M., Jubian, V., and Zou, X. (1989) *J. Am. Chem. Soc. 111*, 186−190.
63. Behrman, E. J., Biallas, M. J., Brass, H. J., Edwards, J. O., and Isaks, M. (1970) *J. Org. Chem. 35*, 3069−3075.
64. Hudson, R. F., and Keay, L. (1960) *J. Chem. Soc.*, 1859−1864.
65. Hudson, R. F. (1965) *Structure and Mechanism in Organophosphorous Chemistry*, Academic Press, New York (253−259).
66. Hays, H. R. (1971) *J. Org. Chem. 36*, 98−101.
67. Kraut, J. (1961) *Acta Crystallogr. 14*, 1146−1152.
68. Ferrier, W. G., Lindsay, A. R., and Young, D. W. (1962) *Acta Crystallogr. 15*, 616.
69. Okaya, Y. (1966) *Acta Crystallogr. 20*, 712−715.
70. Szabo, T., and Stawinski, J. (1995) *Tetrahedron 51*, 4145−4160.
71. Behrman, E. J., Biallas, M. J., Brass, H. J., Edwards, J. O., and Isaks, M. (1970) *J. Org. Chem. 35*, 3063−3069.
72. Leo, A., Hansch, C., and Elkins, D. (1971) *Chem. Rev. 71*, 525−616.
73. Bourne, N., and Williams, A. (1984) *J. Org. Chem. 49*, 1200−1204.
74. Ba-Saif, S., Luthra, A. K., and Williams, A. (1987) *J. Am. Chem. Soc. 109*, 6362−6368.
75. Williams, A. (1992) *Adv. Phys. Org. Chem.*, 1−55.
76. Lowry, T. H., and Richardson, K. S. (1987) *Mechanism and Theory in Organic Chemistry*, 3rd ed. Harper and Row, New York.
77. Hengge, A. C., Tobin, A. E., and Cleland, W. W. (1995) *J. Am. Chem. Soc. 117*, 5919−5926.

BI010801U